



On the development of kinetic models for solvent-free benzyl alcohol oxidation over a gold-palladium catalyst

Federico Galvanin^a, Meenakshisundaram Sankar^b, Stefano Cattaneo^b, Donald Bethell^c, Vivek Dua^{a,*}, Graham J. Hutchings^b, Asterios Gavriilidis^{a,*}

^a Department of Chemical Engineering, University College London, Torrington Place, London WC1E 7JE, UK

^b Cardiff Catalysis Institute, School of Chemistry, Cardiff University, Cardiff CF10 3AT, UK

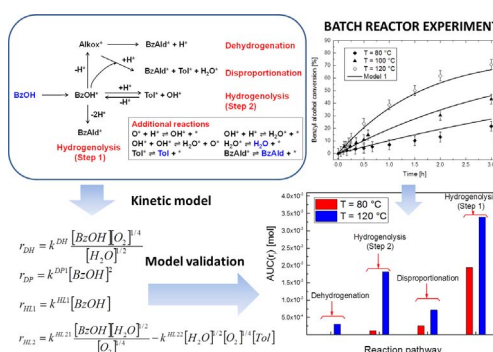
^c Department of Chemistry, University of Liverpool, Liverpool L69 3BX, UK



HIGHLIGHTS

- Simplified kinetic models were developed for benzyl alcohol oxidation.
- Model discrimination was applied to find the most appropriate kinetic model.
- At low temperature, toluene formation is dominated by disproportionation.
- At high temperature, toluene formation is dominated by hydrogenolysis.

GRAPHICAL ABSTRACT



ARTICLE INFO

Keywords:

Alcohol
Aerobic oxidation
Kinetics
Gold-palladium catalyst

ABSTRACT

Bimetallic Au-Pd nanoparticles supported on TiO₂ show excellent catalytic activity and selectivity to benzaldehyde in the solvent-free transformation of benzyl alcohol to benzaldehyde, where toluene is the main observed by-product, together with smaller amounts of benzoic acid, benzyl benzoate and dibenzyl ether. However, despite the industrial relevance of this reaction and importance of tuning the selectivity to the desired benzaldehyde, only a few attempts have been made in the literature on modeling the reaction kinetics for a quantitative description of this reaction system. A kinetic model for the oxidation of benzyl alcohol over Au-Pd is proposed in this paper. The model assumes that hydrogenolysis, disproportionation and dehydrogenation reactions may occur in parallel, and it has been found satisfactory after a model discrimination procedure was applied to a number of simplified candidate models developed from microkinetic studies. Despite its relative simplicity, the proposed model is capable of representing the reactant conversion and distribution of products observed in experiments carried out at different temperature, pressure and catalyst mass in a stirred batch reactor. Major findings include the quantitative evaluation of the impact of hydrogenolysis and disproportionation pathways on benzaldehyde production. At low temperature the disproportionation reaction is the dominant route to toluene formation, while hydrogenolysis dominates at high temperature.

* Corresponding authors.

E-mail addresses: v.dua@ucl.ac.uk (V. Dua), a.gavriilidis@ucl.ac.uk (A. Gavriilidis).

1. Introduction

Benzyl alcohol oxidation is an important alcohol oxidation reaction in industry due to the demand for benzaldehyde as an intermediate in the production of fine chemicals, fragrances and flavouring additives [1]. Stoichiometric oxidants are often used for this transformation, however it is highly desirable to use catalytic systems along with environmentally benign oxidants like O_2 , H_2O_2 or air. Many heterogeneous catalysts have been reported to be active for this transformation, including copper-containing catalysts [2], supported Au [3] and Pd [4,5] monometallic catalysts and Au–Pd bimetallic catalysts [6,7]. The use of inexpensive metals such as Cu, Mn and Ni-containing catalysts also offer a good alternative in comparison with the precious metals, but they are still under study [8,9]. After the discovery that an alloy of Au and Pd leads to a significant enhancement in activity and selectivity by comparison to the Au or Pd mono-metallic catalysts [10], supported Au–Pd catalysts have been extensively used for the oxidation of various alcohols, including benzyl alcohol [11,12]. In particular, Au–Pd nanoparticles supported on TiO_2 have been recently shown to be highly effective in the oxidation of benzyl alcohol [7] exhibiting excellent catalytic activity.

In the oxidation of benzyl alcohol to benzaldehyde using supported Au–Pd catalysts, toluene and water are the main observed by-products, together with benzoic acid, benzyl benzoate and dibenzyl ether [13,14]. Benzaldehyde and benzoic acid are formed by the sequential oxidative dehydrogenation and further oxidation of benzyl alcohol. Dibenzyl ether is formed by the dehydration of benzyl alcohol, while benzyl benzoate is reported to be formed either via hemi-acetal from benzaldehyde or by the esterification of benzoic acid by the substrate [13–16]. However, these products are typically formed in small amounts (< 5%). There are different opinions in the scientific community on the origin of the other main by-product, toluene [12,14,17], which is formed in larger amounts (20–30% depending on the catalyst). Baiker and coworkers [14,16], proposed hydrogenolysis of benzyl alcohol as the origin of toluene using the hydrogen produced from the dehydrogenation of benzyl alcohol. Other groups proposed an alternative disproportionation mechanism of benzyl alcohol [12,17], which results in an equimolar mixture of benzaldehyde and toluene under oxygen-free reacting conditions. However, since under aerobic conditions benzaldehyde is formed by both oxidation as well as disproportionation reactions, it becomes difficult to study the disproportionation reaction alone. A methodology was recently reported to quantify the two reactions separately, even under oxidative conditions [18]. Interestingly, according to this methodology, oxidation and disproportionation reactions seem to have different active sites in the supported Au–Pd catalyst. In particular, metal sites appear to promote the oxidation reaction, while metal–support interface sites promote the disproportionation reaction. Furthermore, the nature of the support was found to be very important for controlling the extent of disproportionation and thus toluene formation [17,18].

In order to describe the concentration of the chemical species involved in the selective oxidation of benzyl alcohol on Au–Pd catalysts in a quantitative way, as well as for catalyst design and process optimisation purposes, a reliable kinetic model is required. Ultimately it is desirable to obtain the most important product, benzaldehyde, in high yield by suppressing the formation of by-products. The kinetic model should implement: *i*) a chemically consistent kinetic mechanism, defining its constitutive rate equations; *ii*) a statistically precise and accurate estimation of the set of kinetic parameters. Despite the great importance of the reaction, only a few attempts have been made to develop kinetic models in order to elucidate the reaction mechanism [17,19,20]. In a recent study [17], a kinetic expression was derived for the solvent-free oxidation of benzyl alcohol on Au–Pd nanoalloys. Two parallel competitive pathways were identified in the gas–liquid–solid

multiphase reaction system as the main source of benzaldehyde: *i*) a direct catalytic oxidative dehydrogenation ($PhCH_2OH + \frac{1}{2}O_2 \rightarrow PhCHO + H_2O$), yielding benzaldehyde and water and this reaction exclusively takes place in the presence of gaseous oxygen; *ii*) a disproportionation reaction ($2PhCH_2OH \rightarrow PhCHO + PhCH_3 + H_2O$), resulting in a equimolar mixture of benzaldehyde, toluene and water occurring both in the presence and the absence of oxygen and thus reducing the selectivity of the desired product, benzaldehyde [17]. Experimental results were obtained in a conventional glass stirred reactor (GSR) operated in a batch mode and the evaluation of kinetics was based on initial reaction rate data. Based on this data set, a kinetic model was proposed that was able to represent in a satisfactory way the data at low conversion, but revealed several limitations on the representation of selectivity at high conversion. More recently, a microkinetic model of benzyl alcohol oxidation over carbon-supported palladium nanoparticles was proposed [20]. The model was able to represent the distribution of by-products such as benzoic acid, benzyl benzoate, and benzyl ether observed in this catalytic system. The same authors extended the same model to the Au–Pd system, again considering carbon-supported nanoparticles [21], observing that using Au–Pd alloying decreased the oxygen adsorption properties relative to pure Pd. The microkinetic model was able to explain the selectivity observed in the catalytic system. However, one practical limitation on the model applicability for reaction engineering purposes is the high number of parameters to be estimated in this model (eleven without considering temperature dependence).

The goal of this paper is to develop a structurally simple kinetic model of benzyl alcohol oxidation over a Au–Pd/ TiO_2 catalyst capable of representing in a quantitative way the experimental observations obtained from a stirred reactor operated in batch mode. A three-step model identification procedure is implemented for this purpose. In the first step, a set of candidate kinetic models is formulated, based on a microkinetic study of plausible reaction mechanisms occurring over the catalyst surface. The complexity of candidate models is reduced to allow a statistically reliable estimation of kinetic parameters from batch reactor data. In the second step, a model discrimination [22] is carried out with the purpose of selecting the most suitable mechanism amongst proposed competitive kinetic models. In the third step, the performance of the best model is tested on a wider range of experimental conditions, in order to investigate the effect of temperature, oxygen pressure and catalyst amount on benzyl alcohol conversion and selectivity to benzaldehyde and toluene. Results show that, despite the relative simplicity of the suggested model, a good agreement with the experimental data is obtained under a wide range of experimental conditions, providing a quantitative representation of the reaction system and elucidating the pathways involved in the production of the main products.

2. Methods

The starting point for the development of the kinetic model is the availability of a chemically consistent reaction mechanism, which cannot be formulated without a precise understanding of the main species present on the catalyst surface. The main precursor species likely to be formed on the catalyst surface from substrate (benzyl alcohol) oxidation [14,19] are illustrated in Fig. 1. Active sites on the catalyst surface remove the benzylic H of benzyl alcohol leading to the formation of the intermediate α -hydroxyalkyl Species 1 (bonded to the catalytic surface through C atoms) and/or the removal of alcoholic H resulting in alkoxy Species 2 (bonded to the catalytic surface through O atoms). These are precursors to the formation of both major products (benzaldehyde and toluene) and the minor by-products [13–16]. Starting from these species on the catalyst surface, several elementary reactions can be considered.

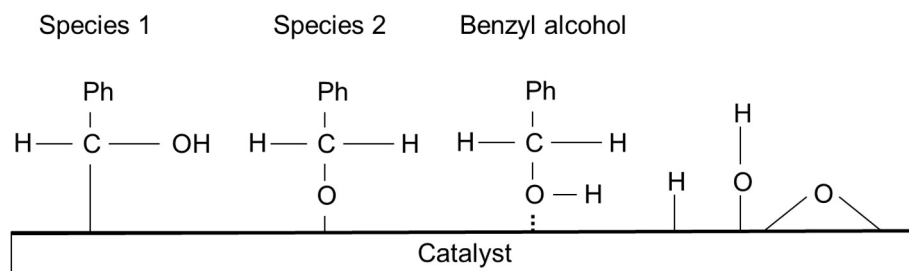


Fig. 1. Species on the catalyst surface.

2.1. Definition of elementary reactions

In an attempt to describe the selective oxidation of benzyl alcohol in a comprehensive way, four main competitive reactions are considered in this study:

1. Dehydrogenation (DH);
2. Hydrogenolysis (HL);
3. Disproportionation (DP);
4. Oxidative Dehydrogenation (ODH).

The **DH** reaction considers the dehydrogenation of precursor species (alkoxy or α -hydroxyalkyl) to benzaldehyde in the form



where $*$ indicates a surface site

The **HL** is a two-step reaction occurring on the catalyst surface involving the breakage of C–OH bonds:

- i) first step (HL1): dehydrogenation of benzyl alcohol to benzaldehyde with the release of hydrogen (Eq. (2))



- ii) second step (HL2): hydrogenolysis of another molecule of benzyl alcohol with the hydrogen from HL1 to form toluene (Eq. (3))



Here the two reactions HL1 and HL2 are separate reactions. One molecule of benzyl alcohol produces one molecule of benzaldehyde and 2H atoms (or 1 molecule of H_2) (HL1) and in the second reaction (HL2) one molecule of toluene is formed from one molecule of benzyl alcohol and the H atoms produced from HL1.

The **DP** is a reaction occurring on the catalyst surface between precursors [17,23] (alkoxy/ α -hydroxyalkyl and benzyl alcohol), which is known to provide an equimolar quantity of toluene and benzaldehyde in the absence of oxygen, according to the following surface reaction:



Unlike the HL reaction, here toluene and benzaldehyde form simultaneously in one step from 2 molecules of benzyl alcohol through a bimolecular reaction where the alkoxy species and the benzyl alcohol are adsorbed closely on the catalyst surface. As illustrated in Fig. 2, two possible mechanisms have been postulated for DP (DP1 and DP2) [23]. In the first step for both mechanisms the substrate adsorbs on the catalyst surface. Depending on the mode of adsorption the proposed mechanism changes. For the first mechanism (DP1) the first molecule of benzyl alcohol adsorbs through the benzylic C after the cleavage of the benzylic C–H bond and the second molecule of benzyl alcohol adsorbs via O of the benzyl alcohol without any bond breaking. For the second mechanism (DP2), the first molecule of benzyl alcohol adsorbs through the alcoholic O after the breaking of the O–H bond and the second benzyl alcohol molecule adsorbs via O of the benzyl alcohol without any bond breaking. After these initial steps a concerted one-step process

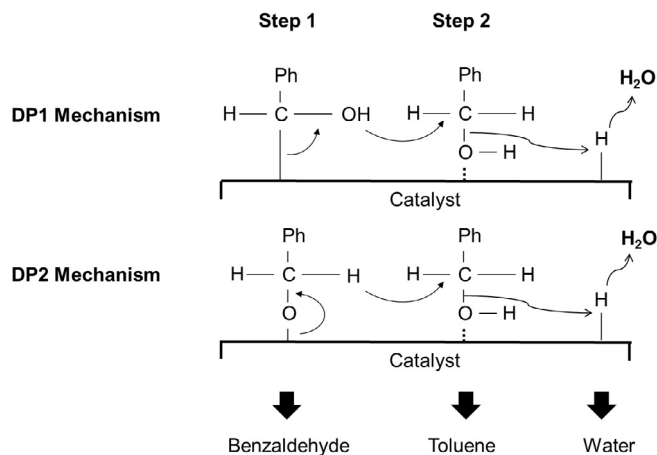


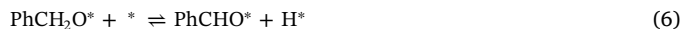
Fig. 2. Two possible mechanisms (DP1 and DP2) for the disproportionation of benzyl alcohol (DP) as reported by Nowicka et al. [23].

involving inter-molecular hydride transfer forms equimolar mixture of benzaldehyde, toluene and water (Fig. 2).

In **ODH** [23,24] oxygen is responsible for benzyl alcohol dehydrogenation by removing water from the catalytic surface through a two-step mechanism. In the first step (oxidation), oxygen subtracts one hydrogen from the substrate via the formation of the alkoxy precursor and OH:



In the second step (dehydrogenation), a second hydrogen from the alkoxy is removed:



The OH^* obtained from Eq. (5) and the hydrogen released from dehydrogenation (Eq. (6)) eventually react on the catalyst surface to produce water. Further oxidation of alkoxy in the presence of OH^* leads to the formation of by-products, like benzoic acid [24]. Among the above-mentioned elementary reactions, DP and HL2 are the only pathways to toluene if hydrogen is present on the catalytic surface, whilst DH, ODH, DP and HL1 routes lead to the formation of benzaldehyde.

2.2. Potential reaction schemes

Starting from the aforementioned elementary reactions, four different models are considered and compared in this study:

- 1) **Model 0** includes benzyl alcohol oxidation ($\text{PhCH}_2\text{OH} + \frac{1}{2}\text{O}_2 \rightarrow \text{PhCHO} + \text{H}_2\text{O}$) (ODH) and disproportionation ($2\text{PhCH}_2\text{OH} \rightarrow \text{PhCHO} + \text{PhCH}_3 + \text{H}_2\text{O}$) (DP) as parallel global reactions, as presented in [17].
- 2) **Model 1** (Fig. 3a) considers DH, DP and HL reactions taking into account the main species on the catalytic surface.
- 3) **Model 2** considers DH, DP and HL2 reaction only (i.e. same scheme

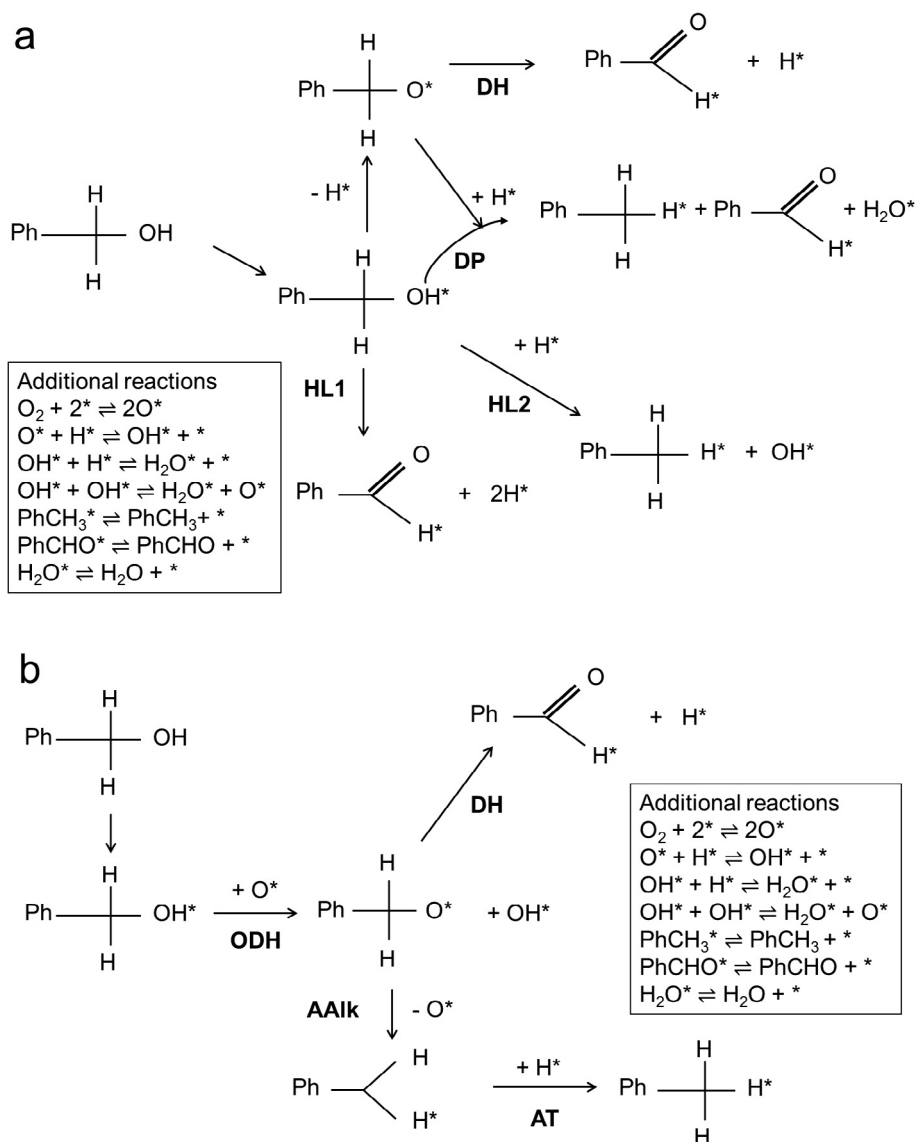


Fig. 3. Reaction schemes considered in the current study: (a) Model 1; (b) Model 3. (*) indicates species adsorbed on the catalyst surface. Additional reactions involving adsorbed O, H and OH species and desorption reactions for main products are included in the schemes. For the sake of clarity, single arrows have been used to denote reversible reactions.

of Model 1 but ignoring the hydrogenolysis pathway HL1, hydrogen used by HL2 is released by DH via alkoxy formation).

4) **Model 3** (Fig. 3b), adapted from Savara et al. [19] where an oxidative dehydrogenation pathway (ODH) is considered and DP reaction is not present. The alkoxy species from ODH can provide benzaldehyde by dehydrogenation on the catalyst surface (DH pathway), or toluene (AT pathway) via the formation of an alkyl intermediate (alkoxy to alkyl AAlk pathway).

In Models 1–3, the following reactions involving H^* and OH^* species are included:



Note that, according to Model 1 and Model 2, oxygen does not directly react with the substrate and/or the alkoxy species (i.e. ODH reaction is not considered), but it has the primary role of removing hydrogen from the catalytic surface. Conversely, direct oxidation reactions (where reaction rate is dependent on oxygen concentration) are considered in both Model 0 and Model 3 reaction schemes. In

particular, according to Model 3, oxygen reacts with the substrate to form the alkoxy species according to ODH reaction.

2.3. Formulation of candidate kinetic models

Model 0: The model presented in [17] was used as a reference model in the current kinetic study of the benzyl alcohol oxidation system. According to Model 0, the benzyl alcohol reaction rate r_{BzOH} is described by the following kinetic expression:

$$-r_{\text{BzOH}} = r_{\text{DP}} + r_{\text{ODH}} = \frac{C[\text{BzOH}]}{K_D^B + [\text{BzOH}]} \left\{ k_{1X} + \frac{k_{2X}[\text{O}_2]}{K_D^O + [\text{O}_2]} \right\} \quad (10)$$

In Eq. (10) r_{BzOH} [mol/s] is the rate of change of concentration of benzyl alcohol (through the parallel DP and ODH reactions with rate of change r_{DP} and r_{ODH} respectively), characterised by the rate coefficients k_{1X} and k_{2X} for the reaction in the absence (DP) and presence (ODH) of O_2 . This model does not capture the enhanced toluene formation in the presence of oxygen [17]. C represents the total number of catalytic sites on the surface, proportional to the weight of catalyst and K_D^O and K_D^B are adsorption constants for oxygen and benzyl alcohol. Note that according to Eq. (10), benzyl alcohol oxidation (through ODH) is

Table 1

Model 1: reaction mechanism. Assumed rate limiting steps are highlighted in bold.

Reaction	Description	Rate and equilibrium equations
$\text{BzOH} + * \rightleftharpoons \text{BzOH}^*$	Benzyl alcohol adsorption	$\theta_{\text{BzOH}^*} = K_1 [\text{BzOH}] \theta_*$
$\text{BzOH}^* + * \rightleftharpoons \text{Alkox}^* + \text{H}^*$	Formation of alkoxy intermediate	$\theta_{\text{Alkox}^*} = K_2 \theta_{\text{BzOH}^*} \theta_*/\theta_{\text{H}^*}$
$\text{Alkox}^* + * \rightleftharpoons \text{BzAld}^* + \text{H}^*$	Dehydrogenation (DH)	$r_{\text{DH}} = k^{\text{DH}} \theta_{\text{Alkox}^*} \theta_* - \frac{k^{\text{DH}}}{K_3} \theta_{\text{BzAld}^*} \theta_{\text{H}^*}$
$\text{Alkox}^* + \text{BzOH}^* + \text{H}^* \rightleftharpoons \text{BzAld}^* + \text{ToI}^* + \text{H}_2\text{O}^*$	Disproportionation (DP)	$r_{\text{DP}} = k^{\text{DP}} \theta_{\text{Alkox}^*} \theta_{\text{BzOH}^*} \theta_{\text{H}^*} - \frac{k^{\text{DP}}}{K_4} \theta_{\text{BzAld}^*} \theta_{\text{ToI}^*} \theta_{\text{H}_2\text{O}^*}$
$\text{BzOH}^* + \text{H}^* \rightleftharpoons \text{ToI}^* + \text{OH}^*$	Hydrogenolysis, step 2 (HL2)	$r_{\text{HL2}} = k^{\text{HL2}} \theta_{\text{BzOH}^*} \theta_{\text{H}^*} - \frac{k^{\text{HL2}}}{K_5} \theta_{\text{ToI}^*} \theta_{\text{OH}^*}$
$\text{BzOH}^* + 2^* \rightleftharpoons \text{BzAld}^* + 2\text{H}^*$	Hydrogenolysis, step 1 (HL1)	$r_{\text{HL1}} = k^{\text{HL1}} \theta_{\text{BzOH}^*} \theta_*^2 - \frac{k^{\text{HL1}}}{K_6} \theta_{\text{BzAld}^*} \theta_{\text{H}^*}^2$
$\text{O}^* + \text{H}^* \rightleftharpoons \text{OH}^* + *$	OH formation	$\theta_{\text{OH}^*} = K_7 \theta_{\text{O}^*} \theta_{\text{H}^*} / \theta_*$
$\text{OH}^* + \text{H}^* \rightleftharpoons \text{H}_2\text{O}^* + *$	Water direct synthesis	$\theta_{\text{H}_2\text{O}^*} = K_8 \theta_{\text{OH}^*} \theta_{\text{H}^*} / \theta_*$
$\text{OH}^* + \text{OH}^* \rightleftharpoons \text{H}_2\text{O}^* + \text{O}^*$	Water from OH	$\theta_{\text{H}_2\text{O}^*} = K_9 \theta_{\text{OH}^*}^2 / \theta_{\text{O}^*}$
$\text{ToI}^* \rightleftharpoons \text{ToI} + *$	Toluene desorption	$\theta_{\text{ToI}^*} = [\text{ToI}] \theta_*/K_{10}$
$\text{BzAld}^* \rightleftharpoons \text{BzAld} + *$	Benzaldehyde desorption	$\theta_{\text{BzAld}^*} = [\text{BzAld}] \theta_*/K_{11}$
$\text{H}_2\text{O}^* \rightleftharpoons \text{H}_2\text{O} + *$	Water desorption	$\theta_{\text{H}_2\text{O}^*} = [\text{H}_2\text{O}] \theta_*/K_{12}$
$\text{O}_2 + 2^* \rightleftharpoons 2\text{O}^*$	Oxygen adsorption	$\theta_{\text{O}^*} = K_{13} [\text{O}_2]^{1/2} \theta_*$

approximately zero order with respect to oxygen, and disproportionation (DP) is approximately zero order with respect to benzyl alcohol. This is consistent with the observed experimental behaviour under solvent-free conditions, when all the catalytic sites are saturated with benzyl alcohol [17].

Models 1 and 2: These were developed starting from a full microkinetic model following a Langmuir-Hinshelwood approach and the mechanism reported in Table 1, under the following assumptions:

- HL1, HL2, DP and DH are competing reactions assumed to take place at the same active sites and represent the (slow) rate limiting steps;
- the adsorption/desorption of products/substrate is very fast;
- the rate limiting steps do not change during the reaction;
- oxygen does not directly react with the substrate (i.e. ODH is not present), but reactions described by Eqs. (7)–(9), involving H^* , O^* and OH^* species (see Section 2.2), are included;
- only benzaldehyde, toluene and water are considered as reaction products.

The last assumption is consistent with the observed experimental results, showing that in the investigated experimental conditions (temperature range $T = 80\text{--}120\text{ }^\circ\text{C}$, pressure range $P = 1\text{--}3\text{ bar}$), only a relatively small amount of other by-products (mainly ester and benzoic acid) is found (always $< 2\%$ in terms of product selectivity).

The expressions for the rate limiting steps are¹:

$$r_{\text{HL1}} = k^{\text{HL1}} \theta_{\text{BzOH}^*} \theta_*^2 - \frac{k^{\text{HL1}}}{K_6} \theta_{\text{BzAld}^*} \theta_{\text{H}^*}^2 \quad (11)$$

$$r_{\text{HL2}} = k^{\text{HL2}} \theta_{\text{BzOH}^*} \theta_{\text{H}^*} - \frac{k^{\text{HL2}}}{K_5} \theta_{\text{ToI}^*} \theta_{\text{OH}^*} \quad (12)$$

$$r_{\text{DP}} = k^{\text{DP}} \theta_{\text{Alkox}^*} \theta_{\text{BzOH}^*} \theta_{\text{H}^*} - \frac{k^{\text{DP}}}{K_4} \theta_{\text{BzAld}^*} \theta_{\text{ToI}^*} \theta_{\text{H}_2\text{O}^*} \quad (13)$$

$$r_{\text{DH}} = k^{\text{DH}} \theta_{\text{Alkox}^*} \theta_* - \frac{k^{\text{DH}}}{K_3} \theta_{\text{BzAld}^*} \theta_{\text{H}^*} \quad (14)$$

where r_i , k_i and K_i are, respectively, the reaction rate, the rate coefficient and the equilibrium constant for the i th limiting step ($i = \text{HL1}, \text{HL2}, \text{DP}, \text{DH}$). Utilizing the equilibrium equations reported in Table 1,

¹ Here and in the following for the sake of conciseness in the kinetic expressions we will use the following notation for reactants and products: *BzOH* for Benzyl Alcohol (PhCH_2OH), *BzAld* for benzaldehyde (PhCHO) and *ToI* for Toluene (PhCH_3).

the coverages θ_i of selected species on the catalyst surface can be computed as a function of measurable quantities (i.e. products/reactants concentrations):

$$\theta_{\text{Alkox}^*} = K_1 K_2 \sqrt{K_7 K_8 K_{12} K_{13}} \frac{[\text{BzOH}][\text{O}_2]^{1/4}}{[\text{H}_2\text{O}]^{1/2}} \theta_* \quad (15)$$

$$\theta_{\text{OH}^*} = \frac{[\text{H}_2\text{O}]^{1/2} \sqrt{K_7 K_8 K_{12} K_{13}} [\text{O}_2]^{1/4}}{K_8 K_{12}} \theta_* \quad (16)$$

$$\theta_{\text{H}_2\text{O}^*} = [\text{H}_2\text{O}] \theta_*/K_{12} \quad (17)$$

$$\theta_{\text{H}^*} = \frac{[\text{H}_2\text{O}]^{1/2}}{\sqrt{K_7 K_8 K_{12} K_{13}} [\text{O}_2]^{1/4}} \theta_* \quad (18)$$

$$\theta_{\text{BzAld}^*} = [\text{BzAld}] \theta_*/K_{11} \quad (19)$$

$$\theta_{\text{ToI}^*} = [\text{ToI}] \theta_*/K_{10} \quad (20)$$

$$\theta_{\text{O}^*} = K_{13} [\text{O}_2]^{1/2} \theta_* \quad (21)$$

$$\theta_{\text{BzOH}^*} = K_1 [\text{BzOH}] \theta_* \quad (22)$$

In Eqs. (15)–(22) the available sites θ_* can be evaluated from $\theta_* = 1 - \sum_{i=1}^{N_{\text{species}}} \theta_i$. The derivation of Eqs. (15)–(18) is reported in the [Supplementary Information](#). The rate expressions of the limiting steps can be rewritten as:

$$r_{\text{HL1}} = k^{\text{HL1}} K_1 [\text{BzOH}] \theta_*^3 - \frac{k^{\text{HL1}}}{K_6 K_7 K_8 K_{11} K_{12} K_{13}} \frac{[\text{BzAld}][\text{H}_2\text{O}]}{[\text{O}_2]^{1/2}} \theta_*^3 \quad (23)$$

$$r_{\text{HL2}} = \frac{k^{\text{HL2}} K_1}{\sqrt{K_7 K_8 K_{12} K_{13}}} \frac{[\text{BzOH}][\text{H}_2\text{O}]^{1/2}}{[\text{O}_2]^{1/4}} \theta_*^2 - \frac{k^{\text{HL2}} \sqrt{K_7 K_8 K_{12} K_{13}}}{K_5 K_{10} K_8 K_{12}} [\text{H}_2\text{O}]^{1/2} [\text{O}_2]^{1/4} [\text{ToI}] \theta_*^2 \quad (24)$$

$$r_{\text{DP}} = k^{\text{DP}} K_1 K_2 [\text{BzOH}]^2 \theta_*^2 - \frac{k^{\text{DP}}}{K_4 K_{10} K_{11} K_{12}} [\text{BzAld}][\text{ToI}][\text{H}_2\text{O}] \theta_*^3 \quad (25)$$

$$r_{\text{DH}} = k^{\text{DH}} K_1 K_2 \sqrt{K_7 K_8 K_{12} K_{13}} \frac{[\text{BzOH}][\text{O}_2]^{1/4}}{[\text{H}_2\text{O}]^{1/2}} \theta_*^2 - \frac{k^{\text{DH}}}{K_3 K_{11} \sqrt{K_7 K_8 K_{12} K_{13}}} \frac{[\text{BzAld}][\text{H}_2\text{O}]^{1/4}}{[\text{O}_2]^{1/4}} \theta_*^2 \quad (26)$$

According to this microkinetic model, oxygen plays a crucial role in balancing the relative extent of HL1 and HL2 reactions. In particular, a high amount of oxygen tends to remove H^* from the catalytic surface, according to Eq. (18), promoting the formation of benzaldehyde through HL1 and DH, and suppressing the formation of toluene through

Table 2
Model 3: reaction mechanism. Assumed rate limiting steps are highlighted in bold.

Reaction	Description	Rate and equilibrium equations
$\text{BzOH} + * \rightleftharpoons \text{BzOH}^*$	Benzyl alcohol adsorption	$\theta_{\text{BzOH}^*} = K_1 [\text{BzOH}] \theta_*$
$\text{O}_2 + 2* \rightleftharpoons 2\text{O}^*$	Oxygen adsorption	$\theta_{\text{O}^*} = K_3 [\text{O}_2]^{1/2} \theta_*$
$\text{BzOH}^* + \text{O}^* \rightleftharpoons \text{Alkox}^* + \text{OH}^*$	Benzyl alcohol oxidative dehydrogenation (ODH)	$\theta_{\text{Alkox}^*} = K_2 \theta_{\text{BzOH}^*} \theta_{\text{O}^*} / \theta_{\text{OH}^*}$
$\text{Alkox}^* + * \rightleftharpoons \text{Alkyl}^* + \text{O}^*$	Alkoxy reduction to Alkyl (AAlk)	$\theta_{\text{Alkyl}^*} = K_4 \theta_{\text{Alkox}^*} \theta_*$
$\text{Alkyl}^* + \text{H}^* \rightleftharpoons \text{Tol}^* + *$	Alkyl to Toluene (AT)	$r_{\text{AT}} = k^{\text{AT}} \theta_{\text{Alkyl}^*} \theta_{\text{H}^*} - \frac{k^{\text{AT}}}{K_5} \theta_{\text{Tol}^*} \theta_*$
$\text{Alkox}^* + * \rightleftharpoons \text{BzAld}^* + \text{H}^*$	Dehydrogenation (DH)	$r_{\text{DH}} = k^{\text{DH}} \theta_{\text{Alkox}^*} \theta_* - \frac{k^{\text{DH}}}{K_6} \theta_{\text{BzAld}^*} \theta_{\text{H}^*}$
$\text{O}^* + \text{H}^* \rightleftharpoons \text{OH}^* + *$	OH formation	$\theta_{\text{OH}^*} = K_7 \theta_{\text{O}^*} \theta_{\text{H}^*} / \theta_*$
$\text{OH}^* + \text{H}^* \rightleftharpoons \text{H}_2\text{O}^* + *$	Water direct synthesis	$\theta_{\text{H}_2\text{O}^*} = K_8 \theta_{\text{OH}^*} \theta_{\text{H}^*} / \theta_*$
$\text{OH}^* + \text{OH}^* \rightleftharpoons \text{H}_2\text{O}^* + \text{O}^*$	Water from OH	$\theta_{\text{H}_2\text{O}^*} = K_9 \theta_{\text{OH}^*}^2 / \theta_{\text{O}^*}$
$\text{BzAld}^* \rightleftharpoons \text{BzAld} + *$	Benzaldehyde desorption	$\theta_{\text{BzAld}^*} = [\text{BzAld}] \theta_* / K_{10}$
$\text{H}_2\text{O}^* \rightleftharpoons \text{H}_2\text{O} + *$	Water desorption	$\theta_{\text{H}_2\text{O}^*} = [\text{H}_2\text{O}] \theta_* / K_{11}$
$\text{Tol}^* \rightleftharpoons \text{Tol} + *$	Toluene desorption	$\theta_{\text{Tol}^*} = [\text{Tol}] \theta_* / K_{12}$

HL2. Furthermore, note that while HL1, HL2 and DH are first order reactions with respect to benzyl alcohol, DP is second order (two benzyl alcohol molecules are required to form one mole of water/toluene/benzaldehyde).

A limitation on the applicability of Model 1 through Eqs. (23)–(26) for reaction engineering purposes is the large number of parameters to be estimated (13 equilibrium constants and 4 rate constants). More importantly, these parameters cannot be uniquely estimated from reactant/product concentration measurements only (i.e. the resulting model is not structurally identifiable [25]). For this reason, a simplification is introduced here with the aim of preserving the estimability of kinetic parameters from batch reactor data. According to Model 1, the following reaction rate expressions for HL1, HL2, DP and DH reactions are derived:

$$r_{\text{HL1}} = k^{\text{HL11}} [\text{BzOH}] - k^{\text{HL12}} \frac{[\text{BzAld}][\text{H}_2\text{O}]}{[\text{O}_2]^{1/2}} \quad (27)$$

$$r_{\text{HL2}} = k^{\text{HL21}} \frac{[\text{BzOH}][\text{H}_2\text{O}]^{1/2}}{[\text{O}_2]^{1/4}} - k^{\text{HL22}} [\text{H}_2\text{O}]^{1/2} [\text{O}_2]^{1/4} [\text{Tol}] \quad (28)$$

$$r_{\text{DP}} = k^{\text{DP1}} [\text{BzOH}]^2 - k^{\text{DP2}} [\text{BzAld}][\text{Tol}][\text{H}_2\text{O}] \quad (29)$$

$$r_{\text{DH}} = k^{\text{DH1}} \frac{[\text{BzOH}][\text{O}_2]^{1/4}}{[\text{H}_2\text{O}]^{1/2}} - k^{\text{DH2}} \frac{[\text{BzAld}][\text{H}_2\text{O}]^{1/4}}{[\text{O}_2]^{1/4}} \quad (30)$$

This model, where reaction rate constants k^i for the i th limiting step are lumped under the hypothesis of constant surface coverage for the species ($\theta_* \rightarrow \text{constant}$), has been found to be structurally identifiable from identifiability test [26], and it only requires 8 parameters to be estimated from experimental data, namely the kinetic parameters for hydrogenolysis step 1 (HL1, parameters k^{HL11} and k^{HL12}), hydrogenolysis step 2 (HL2, parameters k^{HL21} and k^{HL22}), disproportionation (DP, parameters k^{DP1} and k^{DP2}) and dehydrogenation (DH, parameters k^{DH1} and k^{DH2}).

In the development of Model 2, the same reaction rate expressions are employed except Eq. (27) related to the description of HL1 and the model has been found structurally identifiable and requiring only 6 parameters to be estimated from experimental data. For Model 1 the reaction rate expressions for benzyl alcohol is

$$-r_{\text{BzOH}} = r_{\text{HL1}} + r_{\text{HL2}} + 2r_{\text{DP}} + r_{\text{DH}} \quad (31)$$

with r_{HL1} , r_{HL2} , r_{DP} and r_{DH} computed from Eqs. (27)–(30). For Model 2, the pathway HL1 is not present and the corresponding equation becomes

$$-r_{\text{BzOH}} = r_{\text{HL2}} + 2r_{\text{DP}} + r_{\text{DH}} \quad (32)$$

with r_{HL2} , r_{DP} and r_{DH} computed from Eqs. (28)–(30). The reaction rate expressions for all the components are given in the [Supplementary Information](#).

Model 3: The same modelling approach can be extended to the development of Model 3, for which the reaction mechanism is described in Table 2. In this case we assume that the alkoxy species is formed through oxidative dehydrogenation (ODH), while toluene formation is through an alkoxy to alkyl (AAlk) pathway. We also assume that the rate limiting steps are the formation of toluene from alkyl (AT) and the formation of benzaldehyde from alkoxy through dehydrogenation (DH). The expressions for the rate limiting steps are:

$$r_{\text{AT}} = k^{\text{AT}} \theta_{\text{Alkyl}^*} \theta_{\text{H}^*} - \frac{k^{\text{AT}}}{K_5} \theta_{\text{Tol}^*} \theta_* \quad (33)$$

$$r_{\text{DH}} = k^{\text{DH}} \theta_{\text{Alkox}^*} \theta_* - \frac{k^{\text{DH}}}{K_6} \theta_{\text{BzAld}^*} \theta_{\text{H}^*} \quad (34)$$

The coverages of the main species involved in ODH, AAlk, AT and DH reactions are:

$$\theta_{\text{Alkox}^*} = \frac{K_1 K_2 \sqrt{K_3 K_7 K_8 K_{11}} [\text{BzOH}][\text{O}_2]^{1/4}}{K_7 [\text{H}_2\text{O}]^{1/2}} \theta_* \quad (35)$$

$$\theta_{\text{Alkyl}^*} = \frac{K_1 K_2 K_4 \sqrt{K_3 K_7 K_8 K_{11}} [\text{BzOH}]}{K_3 K_7 [\text{H}_2\text{O}]^{1/2} [\text{O}_2]^{1/4}} \theta_* \quad (36)$$

$$\theta_{\text{OH}^*} = \frac{K_3 K_7 [\text{H}_2\text{O}]^{1/2} [\text{O}_2]^{1/4}}{\sqrt{K_3 K_7 K_8 K_{11}}} \theta_* \quad (37)$$

$$\theta_{\text{H}_2\text{O}^*} = [\text{H}_2\text{O}] \theta_* / K_{11} \quad (38)$$

$$\theta_{\text{H}^*} = \frac{[\text{H}_2\text{O}]^{1/2}}{\sqrt{K_3 K_7 K_8 K_{11}} [\text{O}_2]^{1/4}} \theta_* \quad (39)$$

$$\theta_{\text{BzAld}^*} = [\text{BzAld}] \theta_* / K_{10} \quad (40)$$

$$\theta_{\text{Tol}^*} = [\text{Tol}] \theta_* / K_{12} \quad (41)$$

$$\theta_{\text{O}^*} = K_3 [\text{O}_2]^{1/2} \theta_* \quad (42)$$

$$\theta_{\text{BzOH}^*} = K_1 [\text{BzOH}] \theta_* \quad (43)$$

The derivation of Eqs. (35)–(37) and Eq. (39) is reported in the [Supplementary Information](#).

By substituting Eqs. (35)–(43) in Eqs. (33) and (34) the following reaction rate expressions for AT and DH reactions, representing the limiting steps, are derived:

$$r_{AT} = k^{AT} \frac{K_1 K_2 K_4 [BzOH]}{K_3 K_7 [O_2]^{1/2}} \theta_*^2 - \frac{k^{AT}}{K_5 K_{12}} [Tol] \theta_*^2 \quad (44)$$

$$r_{DH} = k^{DH} \frac{K_1 K_2}{K_7} \sqrt{K_3 K_7 K_8 K_{11}} \frac{[BzOH][O_2]^{1/4}}{[H_2O]^{1/2}} \theta_*^2 - \frac{k^{DH}}{K_6 K_{10} \sqrt{K_3 K_7 K_8 K_{11}}} \frac{[BzAlD][H_2O]^{1/2}}{[O_2]^{1/4}} \theta_*^2 \quad (45)$$

The resulting rate expressions with corresponding lumped reaction rate constants k^i ($i = AT, DH$) assuming constant surface coverage for the species ($\theta_* \rightarrow \text{constant}$), are:

$$r_{AT} = k^{AT1} \frac{[BzOH]}{[O_2]^{1/2}} - k^{AT2} [Tol] \quad (46)$$

$$r_{DH} = k^{DH1} \frac{[BzOH][O_2]^{1/4}}{[H_2O]^{1/2}} - k^{DH2} \frac{[BzAlD][H_2O]^{1/2}}{[O_2]^{1/4}} \quad (47)$$

The structurally identifiable model requires the estimation of 4 kinetic parameters from experimental data. Note that a totally different dependence on oxygen is predicted by this model in the pathway AT to toluene formation (as a result of the introduction of the AAlk pathway) for which the rate of reaction (Eq. (46)) is inversely proportional to power 1/2 of the oxygen concentration (while the dependency was 1/4 in Model 1–2, see Eq. (28) for HL2). Only four kinetic parameters need to be estimated, namely the kinetic parameters for alkyl to toluene step (AT, parameters k^{AT1} and k^{AT2}) and dehydrogenation step (DH, parameters k^{DH1} and k^{DH2}). Benzyl alcohol consumption can be evaluated considering the AT and DH reaction rate expressions according to:

$$-r_{BzOH} = r_{DH} + r_{AT} \quad (48)$$

with r_{DH} and r_{AT} described, respectively, by Eqs. (46) and (47). The reaction rate expressions for all the components are given in the [Supplementary Information](#).

2.4. Experimental procedures

2.4.1. Catalyst preparation

HAuCl₄·3H₂O (Sigma Aldrich) and PdCl₂ (Sigma Aldrich) were used as the metal precursors for the synthesis of 1%Au-Pd/TiO₂ catalyst. The catalyst was prepared, with a Au:Pd molar ratio of 1:1, via a previously reported sol-immobilisation method [12,18]. In a typical synthesis, requisite amounts of the aqueous solutions of PdCl₂ and HAuCl₄ were added to 800 mL of double distilled water in a 1 L glass beaker with constant stirring. To this solution, the required amount of a freshly prepared aqueous PVA solution (1 wt%) was added (PVA/(Au + Pd) (wt/wt) = 1.2). After a few minutes of vigorous stirring, the required amount of freshly prepared NaBH₄ solution (0.1 M NaBH₄/(Au + Pd) (mol/mol) = 5) was added to form a dark-brown sol. After 30 min of sol generation, the colloid was immobilized by adding the solid support [TiO₂ (Evonik, P25)] and acidified to pH 1 by concentrated sulphuric acid under vigorous stirring. The amount of support material required was calculated so as to have a total final metal loading of 1 wt%. After 2 h the slurry was filtered, the catalyst washed thoroughly with distilled water (neutral mother liquors) and dried at 120 °C overnight under static air. The filtrate solution was checked for the presence of Au and Pd using Atomic Emission Spectroscopy. It was found that there were no metal ions in the filtrate, indicating that all the metals were immobilized on to the support. A detailed catalyst synthesis procedure can be found in our previous reports [12,18].

2.4.2. Aerobic batch oxidation of benzyl alcohol

Solvent-free aerobic benzyl alcohol oxidation was carried out in a carousel reactor using a 50 mL moderate pressure glass stirred reactor. In a typical reaction, the requisite amount of catalyst and substrate were charged into the reactor at room temperature which was then purged with the required gas (O₂) three times before the reactor was

sealed using a Teflon screw threaded cap. The reactor was always connected to an open gas line to ensure that any gas consumed was replenished. The pressure was measured using a gauge fitted to the gas inlet line. There was no change in the pressure during the course of the reaction. The reactor with the reaction mixture was placed into a pre-heated heating block, which was maintained at the reaction temperature. Switching on the stirring inside the reactor with a magnetic bar at 1000 rpm started the reaction. As will be shown later, no effect on reaction performance was observed when the stirring speed was above 750 rpm. The TiO₂ particles were nonporous, hence internal mass transfer resistances were neglected. After a specific time, the stirring was stopped and the reactor was immediately cooled in an ice bath. After cooling for approx. 10 min, the reactor was opened carefully and the contents were centrifuged. An aliquot of the clear supernatant reaction mixture (0.5 mL) was diluted with mesitylene (0.5 mL) for quantitative analyses in a GC (Varian Star 3800 CX with a 30 m CP-Wax 52 CB column). It was established that no reaction occurred in the absence of the Au–Pd catalyst or in the presence of the catalyst support alone.

2.5. Kinetic modelling

The batch reactor was modelled through a system of differential and algebraic equations (DAEs) in the form:

$$\frac{dC_j}{dt} = \frac{\sum_{i=1}^{N^{Reac}} \nu_{ij} \alpha r_{ij}}{m_s} \quad (49)$$

where C_j is the j th component concentration [mol/kg] (benzyl alcohol, benzaldehyde, water, toluene), r_{ij} is the i th reaction rate [mol/s] with respect to the j th component, m_s is the substrate mass [kg], ν_{ij} is the stoichiometric coefficient of the j th species in the i th reaction (negative for reactants and positive for the product species) and α is a factor introduced to account for the amount of catalyst used in the reaction system. α is evaluated from

$$\alpha = \frac{m_{cat}}{m_{cat}^0} \quad (50)$$

where m_{cat} is the catalyst mass [g] and m_{cat}^0 is a reference catalyst mass $m_{cat}^0 = 0.020$ g which is the amount of catalyst used in the reference experiments. Oxygen is assumed to be present in the liquid phase at its equilibrium concentration

$$C_{O_2} = \frac{P_{O_2}}{K^H} C_{BzOH} \quad (51)$$

where P_{O_2} is the oxygen pressure [bar] and K^H is the Henry constant [bar] obtained from the following correlation [27]

$$\ln(K^H) = A + \frac{B}{T} \quad (52)$$

where $A = 7.39$ and $B = 228$. The values of the equilibrium oxygen concentration at different temperatures are given in the [Supplementary Information](#). The reaction rate constants k_i in each reaction rate expression were evaluated using a modified Arrhenius equation in the form:

$$k_i = \exp \left[\ln(A_i) - \frac{E_a^i}{RT} \right] = \exp \left[\theta_{1,i} - \frac{\theta_{2,i}}{T} \right] \quad i = 1 \dots N^{Reac} \quad (53)$$

where N^{Reac} is the number of reactions taking place. This form was used with the purpose of preserving the structural identifiability of candidate kinetic models [25,26] by minimising the impact of parameter correlation during the estimation of parameters E_a^i (activation energies) and A_i (pre-exponential factors) by estimating $\theta_{1,i} = \ln(A_i)$ and $\theta_{2,i} = E_a^i/R$ [28]. gPROMS ModelBuilder [29] was used as simulation software for the integration of the system of differential and algebraic equations described by Eqs. (49)–(53) with the following expressions for reaction rates: Eq. (10) for Model 0; Eqs. (27)–(30) for Model 1; Eqs. (28)–(30)

for Model 2; Eqs. (46) and (47) for Model 3. The software was also used for the estimation of kinetic parameters and for the statistical assessment of model adequacy. The precision in the estimation of kinetic parameters was evaluated in terms of the t -test. For a statistically precise estimation, the t -value of the i th kinetic parameter (at 95% confidence level) is

$$t_i = \frac{\hat{\theta}_i}{2\sqrt{v_i^{\hat{\theta}}}} \quad (54)$$

and should be higher than t^{ref} , a reference t -value given by a Student t -distribution with $(N - N_{\theta})$ degrees of freedom (N is the total number of experimental points while N_{θ} is the number of model parameters). In Eq. (54) $\hat{\theta}_i$ is the estimated value $v_i^{\hat{\theta}}$ is the estimated variance of the i th kinetic parameter obtained from maximum likelihood parameter estimation [30]. Maximum likelihood parameter estimation was carried out with simple bounds on parameters using an SRQPD optimisation solver to solve the nonlinear optimisation problem; the solver DASOLV was used for the integration of the DAEs. A two-step parameter estimation procedure was applied starting from multiple initial guesses to mitigate the risk of incurring into local minima: in the first step (i), parameters $\theta_{1,i}$ were estimated by fixing $\theta_{2,i}$; in the second step (ii), parameters $\theta_{2,i}$ were estimated by fixing $\theta_{1,i}$. For Model 1 the i -ii) iterative procedure involved a total CPU time of approximately 10 min on a Intel® Core Xeon® E5-1650, 3.5 GHz, RAM 8 GB.

The quality of fitting (model adequacy) was assessed for each candidate kinetic model by using a chi-square (χ^2) test. For each model the global chi-square χ_{Glob}^2

$$\chi_{Glob}^2 = \sum_{i=1}^{N_y} \chi_i^2 = \sum_{i=1}^{N_y} \sum_{j=1}^{N_{sp}} \frac{(y_{ij} - \hat{y}_{ij})^2}{\sigma_{y_i}^2} \quad (55)$$

was computed and compared with χ_{Ref}^2 , a tabulated reference value from a χ^2 distribution with $(N - N_{\theta})$ degrees of freedom, where N is the total number of experimental points and N_{θ} is the number of model parameters at 95% confidence level. In Eq. (55) y_{ij} is the j th observation of the i th measured response, \hat{y}_{ij} is the relative model prediction, N_{sp} is the number of samples for each measured response, N_y is the number of measured responses, while χ_i^2 and $\sigma_{y_i}^2$ are the chi-square and the expected variance for the i th measured response respectively. The best model in terms of fitting performance is the model with the lowest value of χ_{Glob}^2 and, if $\chi_{Glob}^2 < \chi_{Ref}^2$, the chi-square test is passed and the model provides an adequate representation of experimental data. In the current study, the experimental observations used for model development were measurements of benzyl alcohol conversion (X)

$$X = \frac{C_{BzOH,in} - C_{BzOH,j}}{C_{BzOH,in}} 100\% \quad (56)$$

and selectivity to benzaldehyde (S^{BzAlD}) and toluene (S^{Tol}) in the form

$$S^i = \frac{C_{i,j} \nu}{C_{BzOH,in} X} 100\% \quad (57)$$

In Eqs. (56) and (57) $C_{BzOH,in}$ and $C_{BzOH,j}$ are, respectively, the initial concentration of benzyl alcohol and the concentration in the j th collected sample, $C_{i,j}$ is the i th product concentration in the j th sample and ν is the number of alcohol moles required to produce one mole of i th product. The observed variability in the measurements, obtained from 3 repeated experiments, is given by $\sigma_{y,X} = 1.3\%$ and $\sigma_{y,S^i} = 1\%$. The global chi-square (Eq. (55)) was used for a quantitative comparison of the relative performance of candidate kinetic models as well as for model discrimination purposes [22].

3. Results

3.1. Set of experiments performed

The set of experiments carried out in the batch reactor is illustrated in Table 3. The main goal of the experimental study was to investigate the effect of a change in temperature, pressure, stirring speed and amount of catalyst on benzyl alcohol conversion and selectivity to benzaldehyde and toluene. Reference experimental conditions were $T = 80$ °C, $P = 1$ bar, $m_{cat} = m_{cat}^0 = 0.020$ g, $m_s = 1$ –2 g, 1000 rpm stirring speed. Experiments at different stirring speed (SS1-5) were carried out to verify the absence of external mass transfer limitations in the reactor at both $T = 80$ °C and $T = 120$ °C ($P_{O_2} = 1$ bar). At $T = 80$ °C, the change in conversion and selectivity passing from 500 to 1000 rpm was negligible. At $T = 120$ °C, again no significant change in conversion was observed (i.e. the variation was $< 2\%$) passing from 750 to 1000 rpm stirring speed, and no effect was observed on selectivity. All the experiments used for the determination of reaction kinetics were performed at 1000 rpm. The carbon balance in the performed experiments was always higher than 96%.

3.2. Model discrimination from reference experiment R1

A preliminary model discrimination, based on statistical indexes was carried out based on the reference experiment R1 ($T = 80$ °C, $P_{O_2} = 1$ bar, $m_s = 2$ g, $m_{cat} = 0.020$ g). Results in terms of fitting the candidate kinetic models (Model 0–3) to benzyl alcohol conversion,

Table 3

Experiments for the development of kinetic models of benzyl alcohol oxidation. All experiments were performed with a 1% Au-Pd/TiO₂ sol-immobilised catalyst.

Experiment ID	Description	Experimental conditions				
		T [°C]	m_{cat} [g]	P_{O_2} [bar]	m_s [g]	Stirring sped [rpm]
R1	Reference experiment	80	0.020	1	2	1000
R2	Reference experiment	80	0.020	1	1	1000
T1,T1b (replicate)	Temperature effect	100	0.020	1	1	1000
T2,T2b (replicate)	Temperature effect	120	0.020	1	1	1000
T3	Temperature effect	140	0.020	1	1	1000
C1	Effect of catalyst amount	80	0.010	1	1	1000
C2	Effect of catalyst amount	80	0.004	1	1	1000
C3	Effect of catalyst amount	80	0.080	1	1	1000
C4	Effect of catalyst amount	120	0.010	1	1	1000
C5	Effect of catalyst amount	120	0.040	1	1	1000
C6	Effect of catalyst amount	120	0.005	1	1	1000
P1	Pressure effect	80	0.020	3	1	1000
P2	Pressure effect	80	0.020	2	1	1000
P3	Pressure effect	80	0.020	1	1	1000
SS1	Effect of stirring speed	80	0.020	1	1	500,1000
SS2-5	Effect of stirring speed	120	0.020	1	1	300,500,750,1000

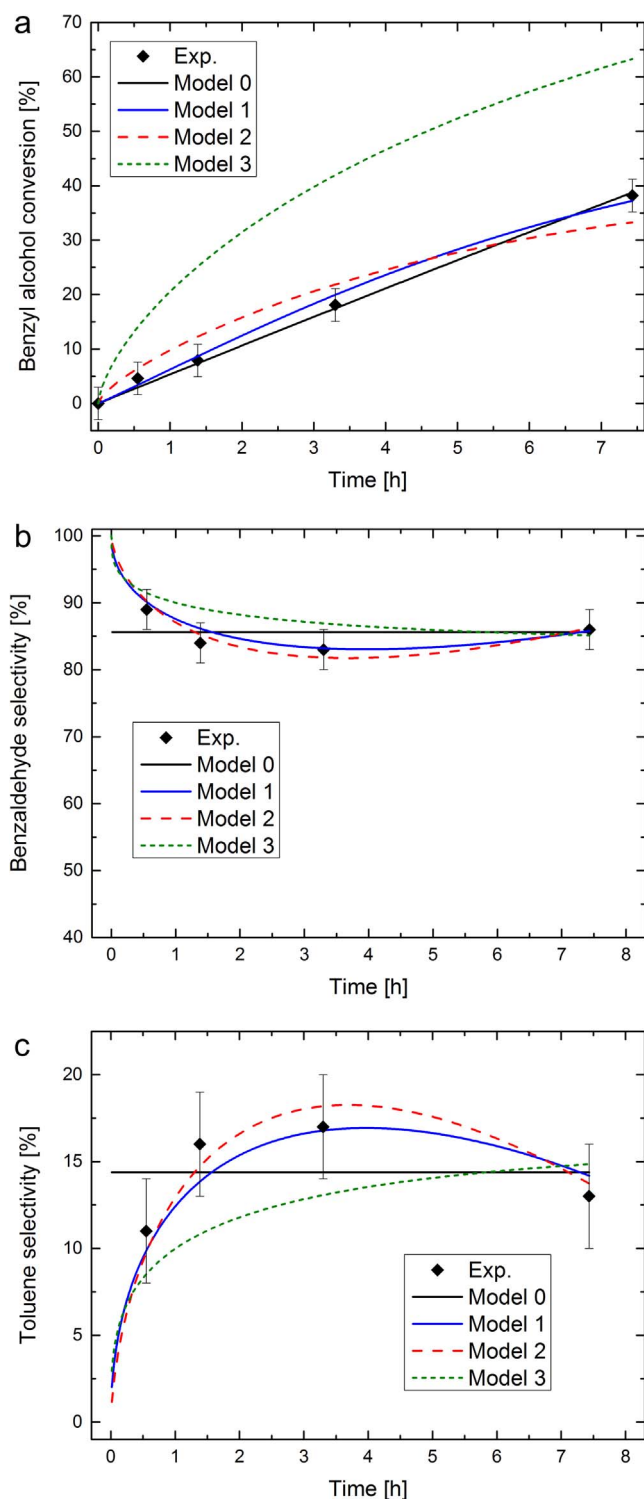


Fig. 4. Simulation profiles obtained after preliminary model discrimination from reference experiment ($T = 80\text{ }^{\circ}\text{C}$, $P_{\text{O}_2} = 1\text{ bar}$, $m_s = 2\text{ g}$, $m_{\text{cat}} = 0.020\text{ g}$): (a) benzyl alcohol conversion; (b) selectivity to benzaldehyde; (c) selectivity to toluene. The experimental points are indicated by black diamonds.

benzaldehyde selectivity and toluene selectivity data are illustrated in Fig. 4. Experimental data showed a nearly linear increase of benzyl alcohol conversion with time, reaching about 38% after 7 h (Fig. 4a). Selectivity to benzaldehyde was always higher than 80% (Fig. 4b) and exhibited a minimum due to a maximum on formation of toluene after around 3 h (Fig. 4c). Under these experimental conditions, the main products observed were benzaldehyde and toluene (only traces of

Table 4

Model discrimination in terms of χ^2 statistics (values indicating model inadequacy are highlighted in bold). The lowest value of global χ^2 , corresponding to the best model, is underlined.

Model	χ^2_{Conv}	χ^2_{BzAld}	χ^2_{STol}	χ^2_{Glob}
Model 0	0.415	2.341	2.534	5.291
Model 1	0.719	0.671	0.349	<u>1.739</u>
Model 2	6.752	0.521	0.598	7.871
Model 3	22.012	3.592	3.702	29.306
χ^2_{Ref}				3.652

benzoic acid and benzyl benzoate were detected). It is apparent from Fig. 4 that the four models predict conversion and selectivity profiles in a very different way:

- Model 0 provides a good representation of conversion, but it can only represent an average (constant) value for benzaldehyde and toluene selectivity during the experiment; hence, it cannot be used for representing the distribution of products in the reactor at different reaction times in a quantitative way;
- Model 1 provides a good representation of both conversion and selectivity;
- Model 2 provides a good representation of selectivity, but a poor representation of conversion;
- Model 3 overestimates conversion, and selectivity is well represented only at the end of the experiment.

Model 2 is not able to represent the conversion in a very reliable way, but is capable of representing toluene and benzaldehyde selectivity. Model 3 predicts a higher conversion as a result of the AT pathway to toluene formation (Eq. (46)), which is defined by the oxidative dehydrogenation (ODH) step to alkoxy formation and the subsequent conversion of the alkoxy to alkyl. Selectivity is also not properly represented during the experiment. In particular, the model is not capable of representing the experimentally observed maximum on toluene formation. Comparing Model 1 and Model 2 performance on conversion, it seems that the introduction of the direct HL1 pathway in the kinetic scheme plays an important role under these experimental conditions, as it greatly improves the description of conversion. Results in terms of χ^2 statistics obtained after values for k_i were estimated for each candidate model are reported in Table 4. In order to ensure that the results obtained are due to the inherent model structure and not due to artificial numerical convergence the parameter estimation procedure was carried starting from stochastically generated points in the parameter space in order to mitigate the risk of incurring local minima. The estimated values of kinetic parameters for each model are reported in the Supplementary Information.

As it is clear from the results of Table 4, Model 0 and Model 1 provide the best representation of conversion but, as previously discussed, only Model 1 can be used for representing the distribution of products (i.e. selectivity) at different reaction times. Both Model 2 and Model 3 are not adequate to represent the experimental observations under reference conditions. Hence, based on the relative fitting performance of candidate models, the model with the lowest global chi-square (Model 1) was selected as the most suitable candidate for representing the observations under a wider range of experimental conditions. This model was also the only one found adequate to represent the system according to the χ^2 test (i.e. $\chi^2_{\text{Glob}} < \chi^2_{\text{Ref}}$).

3.3. Evaluation of model 1 performance under different experimental conditions

Model 1 performance was assessed by fitting the model to experiments under different experimental conditions; these include:

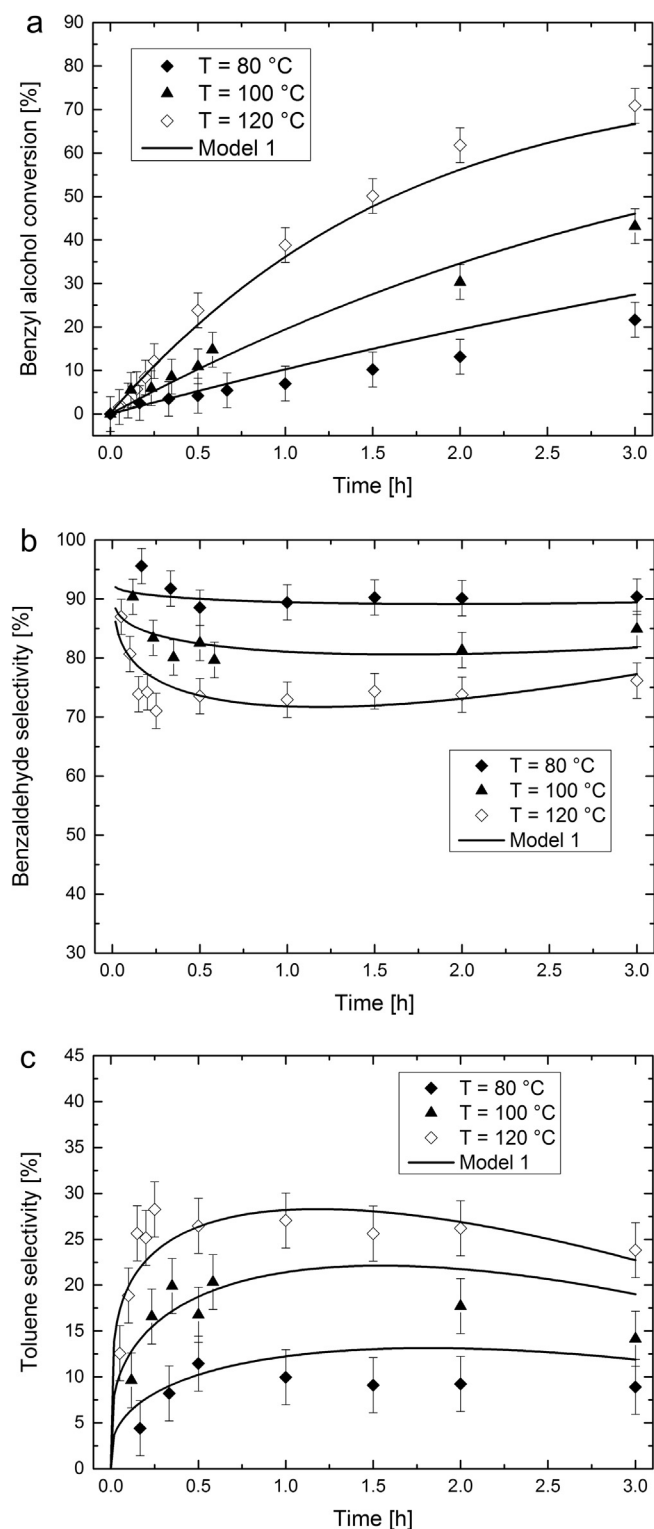


Fig. 5. Investigation of temperature effect ($T = 80$ – 120 °C): (a) effect on benzyl alcohol conversion; (b) effect on selectivity to benzaldehyde; (c) effect on selectivity to toluene. Solid lines represent the model performance at different reaction temperatures. Experiments were carried out at $m_{\text{cat}} = 0.02$ g, $P_{\text{O}_2} = 1$ bar, $m_s = 1$ g.

- Temperature (experiments T1, T1b, T2, T2b, T3);
- Pressure (experiments P1, P2, P3);
- Catalyst amount (experiments C1 to C6).

Results are detailed in the following sections for Model 1 only for the sake of conciseness. Nonetheless, it was verified that Model 0,

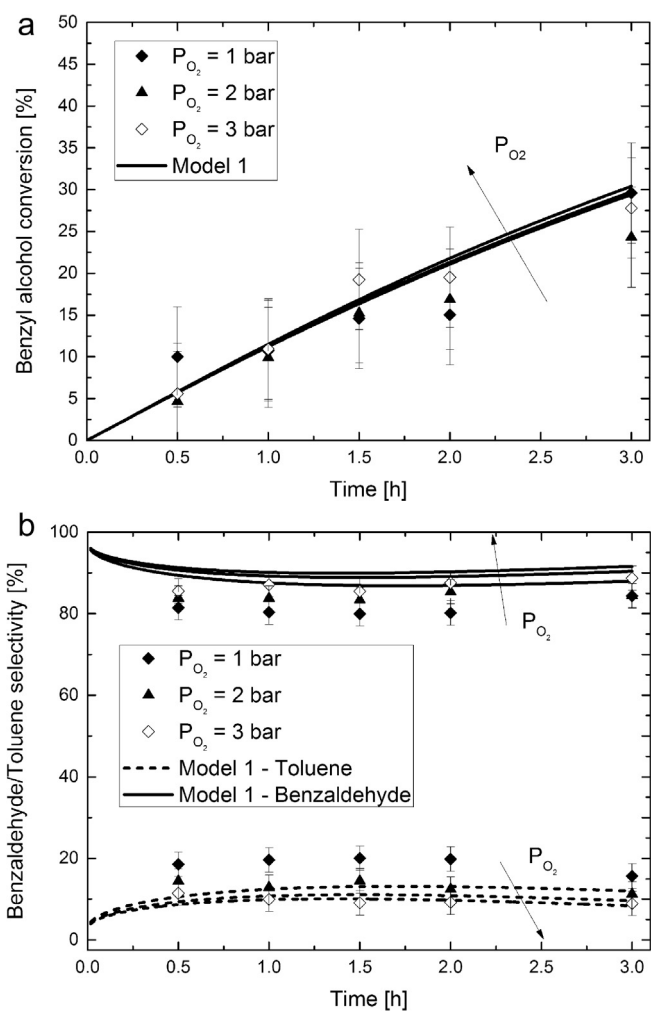


Fig. 6. Investigation of oxygen pressure effect ($P_{\text{O}_2} = 1$ – 3 bar): (a) effect on benzyl alcohol conversion; (b) effect on selectivity to benzaldehyde and toluene. Solid and broken lines represent the model performance. Experiments were carried out at $m_{\text{cat}} = 0.02$ g, $T = 80$ °C, $m_s = 1$ g.

Model 2 and Model 3 showed the same limitations on the representation of system concentrations described in Section 3.2 even when applied to investigate different conditions of temperature, pressure and catalyst amount.

3.3.1. Temperature effect

An increase in temperature provides a progressive increase in benzyl alcohol conversion (Fig. 5a). Interestingly, the quasi-linear behaviour observed at low temperatures ($T = 80$ °C) is lost at high temperatures. The highest conversion (70%) is observed at $T = 120$ °C and 3 h. However, increasing the temperature decreases the selectivity to the desired product, benzaldehyde (Fig. 5b) and promotes the formation of toluene (Fig. 5c). The model is able to represent in a very reliable way both the conversion and selectivity at various temperatures, with only a slight over-estimate of conversion at $T = 80$ °C.

3.3.2. Pressure effect

The effect of pressure on conversion and selectivity observed in experiments P1–P3 is more difficult to interpret as these experiments are affected by higher uncertainty in the concentration measurements due to the presence of acetal (derived from benzaldehyde) forming in the reaction system. According to Fig. 6a, at low reaction times (under 1 h) oxygen pressure seems to increase the conversion. However, after 3 h, all the experiments at higher pressures ($P_{\text{O}_2} = 2$ and $P_{\text{O}_2} = 3$ bar) exhibited approximately the same benzyl alcohol conversion

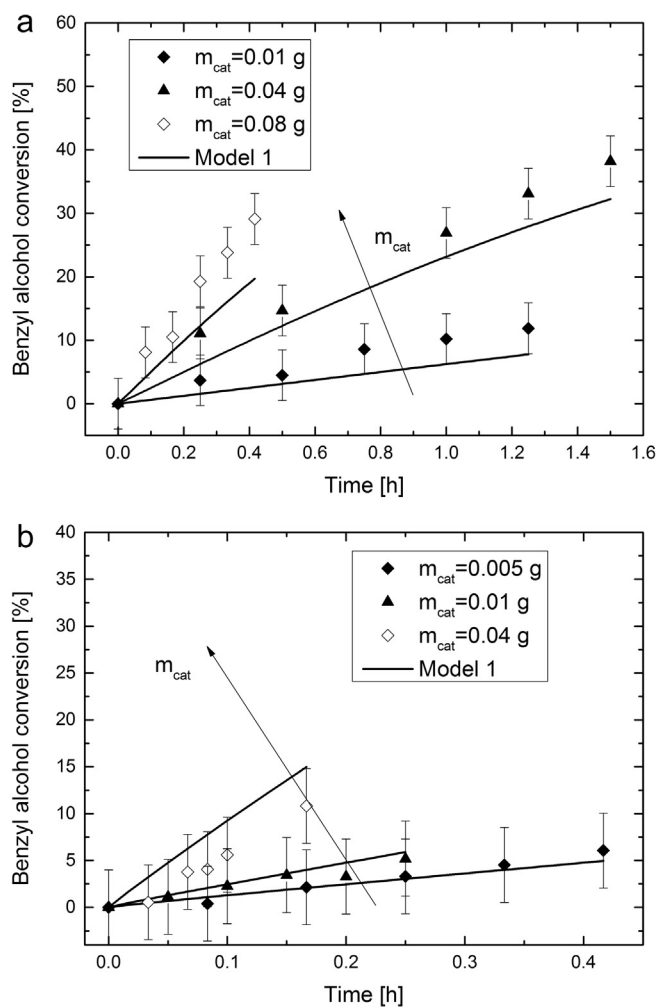


Fig. 7. Effect of catalyst amount on benzyl alcohol conversion at different temperatures: (a) $T = 80\text{ }^{\circ}\text{C}$ ($m_{\text{cat}} = 0.01\text{--}0.08\text{ g}$); (b) $T = 120\text{ }^{\circ}\text{C}$ ($m_{\text{cat}} = 0.005\text{--}0.04\text{ g}$). Solid lines represent the model performance. Experiments were carried out at $P_{\text{O}_2} = 1\text{ bar}$, $m_s = 1\text{ g}$.

($X = 25\text{--}30\%$ against $X = 20\%$ of the reference experiment). Because of the greater uncertainty in the values of measurements in these experiments, the model is not able to capture this sudden increment of conversion, but provides a conversion of around 23% at higher pressures after 2 h. An even higher degree of uncertainty is also present in the experimental characterisation of selectivity (Fig. 6b) where again the results observed at $P_{\text{O}_2} = 2$ and $P_{\text{O}_2} = 3$ bar do not differ much. The model is capable of representing the increase in benzaldehyde selectivity observed at higher pressures (after 3 h $S^{\text{BzAld}} \approx 90\text{--}92\%$ at $P_{\text{O}_2} = 2\text{--}3$ bar), but tends to under-estimate toluene formation at low pressure.

3.3.3. Effect of catalyst amount

The effect of catalyst mass m_{cat} on conversion and selectivity to products was assessed at both low ($T = 80\text{ }^{\circ}\text{C}$) and high ($T = 120\text{ }^{\circ}\text{C}$) reaction temperatures. The results are given in Fig. 7 for benzyl alcohol conversion. The model, even if it tends to underestimate the conversion at low temperature (i.e. see for example experiment C3, $m_{\text{cat}} = 0.08\text{ g}$, high amount of catalyst), is capable of representing the increase of conversion observed in the experiments for increasing catalyst amount. Most importantly, it can represent the distribution of products in a reliable way. Selectivity results for experiments C1, C2 and C3 are reported in Fig. 8. Notwithstanding the presence of some uncertainty in the measurements,

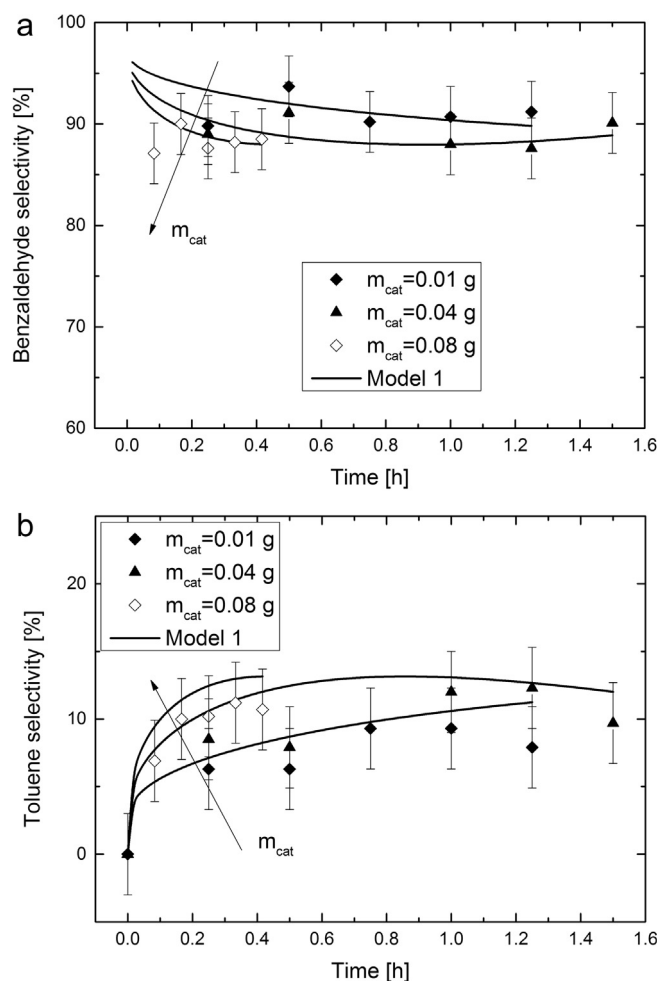


Fig. 8. Effect of catalyst amount on selectivity ($T = 80\text{ }^{\circ}\text{C}$, $P_{\text{O}_2} = 1\text{ bar}$, $m_s = 1\text{ g}$): (a) effect on selectivity to benzaldehyde; (b) effect on selectivity to toluene. Solid lines represent the model performance.

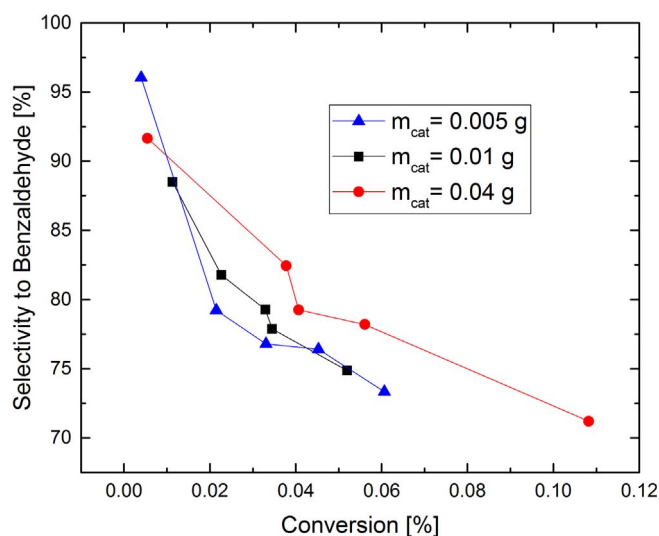


Fig. 9. Effect of conversion on selectivity to benzaldehyde at $T = 120\text{ }^{\circ}\text{C}$ for variable catalyst amount ($m_{\text{cat}} = 0.005\text{--}0.04\text{ g}$). Experiments were carried out at $P_{\text{O}_2} = 1\text{ bar}$, $m_s = 1\text{ g}$.

Table 5

Results from parameter estimation in terms of estimated value, 95% confidence interval and *t*-values. Upper and lower bounds of variability for model parameters, defining the preliminary parameter uncertainty domain used in parameter estimation, are reported. For a statistically precise parameter estimation of the parameter, the *t*-value of the parameter should be greater than the reference *t*-value reported in bold.

Model parameter	Final value	Upper/Lower bounds	Confidence interval 95%	95% <i>t</i> -value
E_a^{HL11} [J/mol]	29623	1.0E3–1.0E5	± 6568	4.51
E_a^{HL12} [J/mol]	–	–	–	–
E_a^{HL21} [J/mol]	58358	1.0E3–1.0E5	± 15817	3.69
E_a^{HL22} [J/mol]	97766	1.0E3–1.0E5	± 33948	2.88
E_a^{DP1} [J/mol]	55520	1.0E3–1.0E5	± 32369	1.71
E_a^{DP2} [J/mol]	–	–	–	–
E_a^{DH1} [J/mol]	76360	1.0E3–1.0E5	± 19044	4.01
E_a^{DH2} [J/mol]	–	–	–	–
A_{HL11} [s ⁻¹]	6.916E3	1.0E–5–1.0E9	± 1.655E3	4.17
A_{HL12} [s ⁻¹ (mol/kg) ^{1/4}]	4.540E–5	–	–	–
A_{HL21} [s ⁻¹ (mol/kg) ^{1/2}]	6.108E6	1.0E–5–1.0E9	± 1.965E6	3.11
A_{HL22} [s ⁻¹ (mol/kg) ^{3/4}]	1.184E2	1.0E–5–1.0E9	± 3.761E1	3.15
A_{DP1} [s ⁻¹ (mol/kg)]	1.558E5	1.0E–5–1.0E9	± 7.212E4	2.16
A_{DP2} [s ⁻¹ (mol/kg) ²]	4.540E–5	–	–	–
A_{DH1} [s ⁻¹ (mol/kg) ^{-1/4}]	7.429E8	1.0E–5–1.0E9	± 2.769E8	2.66
A_{DH2} [s ⁻¹]	4.540E–5	–	–	–
Reference <i>t</i>-value (95%):				1.65

the model is able to represent the experimentally observed decrease in benzaldehyde selectivity due to higher conversion for increasing amount of catalyst. This observed behaviour is apparent at high temperatures (Fig. 9). A low amount of catalyst tends to provide a low conversion (only around $X \approx 10\%$ after 1.2 h), which positively influences the selectivity towards the desired product, as clearly shown in Fig. 8a.

3.4. Estimation of kinetic parameters

Results from the estimation of kinetic parameters from reference experiments and experiments at different temperature, pressure and catalyst amount are given in Table 5, and provide some further insight. Due to the simplifying modelling assumptions (see Section 2.3), confidence intervals obtained from the fitting must be interpreted with some caution for multi-parameter estimation purposes. The relatively low value of the activation energy for HL1 suggests a strong affinity of the catalyst towards hydrogen, as the dehydrogenation step represents

the preferential pathway to benzaldehyde formation. However, also the DH mechanism (via alkoxy) seems to be present, with corresponding activation energy well below 90 J/kmol, in agreement with the values obtained by Savara et al. [20], although a different catalyst (Pd/C) was used in their study. The model shows that both disproportionation (DP) and hydrogenolysis (HL2) pathways are present, the latter representing the main route to toluene at higher temperatures. This is in contrast with the mechanism proposed by the same authors where only a dehydrogenation mechanism via benzyl was suggested to explain toluene formation. The kinetic parameters A_i related to HL1, DP and DH inverse reactions are negligible ($\ln(A_i) = -10$, corresponding to $A_i \approx 4.540E-5$) so that these reactions can be ignored and the corresponding activation energies have not been estimated. Hence, the kinetic model described by Eqs. (27)–(30) can be further simplified to

$$r_{HL1} = k^{HL1} [BzOH] \quad (58)$$

$$r_{HL2} = k^{HL21} \frac{[BzOH][H_2O]^{1/2}}{[O_2]^{1/4}} - k^{HL22} [H_2O]^{1/2} [O_2]^{1/4} [Tol] \quad (59)$$

$$r_{DP} = k^{DP1} [BzOH]^2 \quad (60)$$

$$r_{DH} = k^{DH} \frac{[BzOH][O_2]^{1/4}}{[H_2O]^{1/2}} \quad (61)$$

The resulting reaction scheme is given in Fig. 10. The parameter estimation is statistically satisfactory for the full set of kinetic model parameters (i.e. the *t*-values are higher than the reference *t*-value). Furthermore, the kinetic model described by rate Eqs. (58)–(61) provides a good fitting of the full set of experiments as underlined by the chi-square statistics:

$$\chi_{Glob}^2 = 269.2 < 276.1 = \chi_{Ref}^2 \quad (62)$$

The global chi-square (χ_{Glob}^2) is lower than the reference chi-square (χ_{Ref}^2), meaning that the model is adequate for representing the selected set of experiments. However, it has to be pointed out that the assumption of constant coverage θ_* in the formulation of the simplified models might represent a potential source of uncertainty affecting the estimation of kinetic parameters and the statistical quality of fitting. Furthermore, it is also possible that some rate limiting steps change during the course of reaction. This might explain the difference observed between the models and the experiments at some investigated experimental conditions.

The model allows for a quantitative evaluation and comparison of the four parallel limiting steps proposed in the formulation of Model 1 kinetic mechanism. The relative importance of each reaction can be evaluated by computing the area under the curve of reaction rate

$$AUC(r_i) = \int_0^\tau r_i dt \quad i = HL1, HL2, DP, DH \quad (63)$$

where the integration horizon τ has been fixed to $\tau = 2.5$ h. According

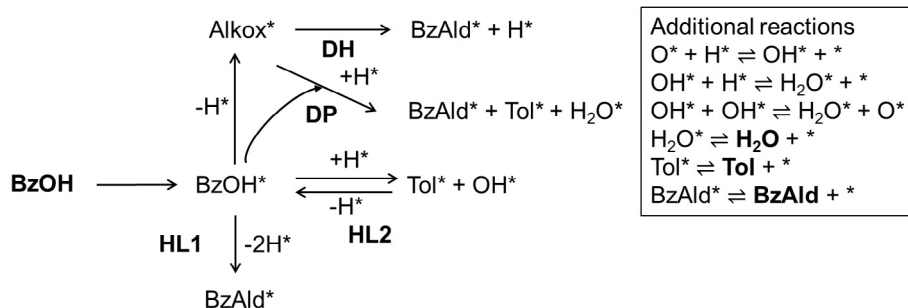


Fig. 10. Reaction scheme determined after model identification from experimental data (* stands for intermediate species on the catalyst surface; observable species are highlighted in bold).

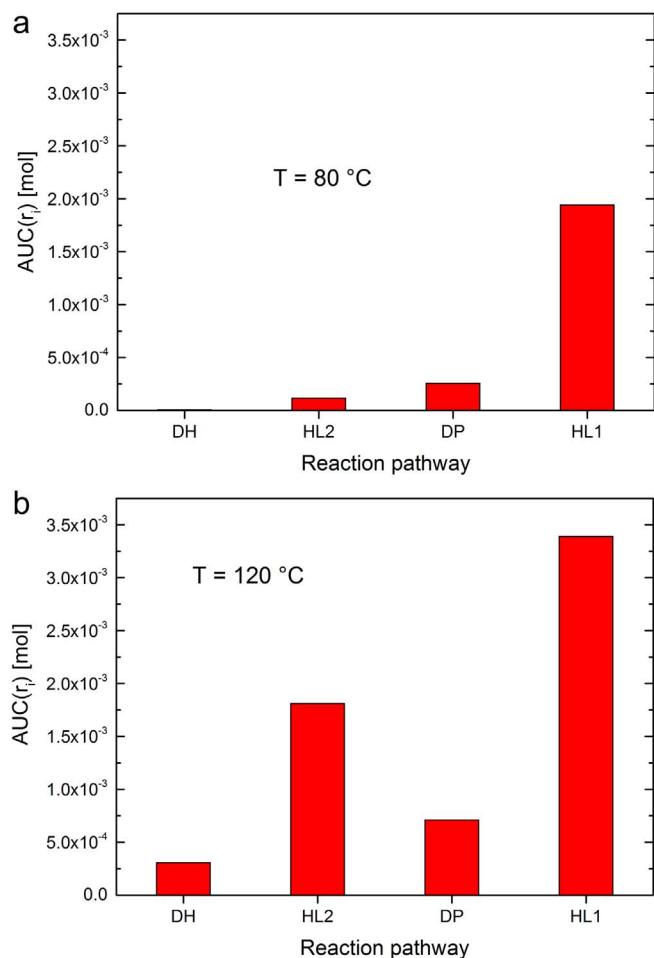


Fig. 11. Analysis of reactions in terms of $AUC(r_i)$ at different temperatures ($P_{O_2} = 1$ bar, $m_s = 1$ g, $m_{cat} = 0.020$ g): (a) $T = 80$ °C; (b) $T = 120$ °C.

to the model, at low temperatures ($T = 80$ °C) (Fig. 11a), solely the hydrogenolysis reaction HL1 leads to benzaldehyde, while disproportionation (DP) (rather than hydrogenolysis via HL2) seems to be the preferential pathway to toluene. Only a limited amount of toluene is provided by hydrogenolysis pathway HL2, and this appears to support the existence of a bimolecular disproportionation route to toluene at low temperatures. Furthermore, it is interesting to notice that dehydrogenation pathway DH is not present at all at low temperature, suggesting a further potential simplification of the model at these experimental conditions. At high temperatures ($T = 120$ °C) (Fig. 11b) the situation is very different. The role of hydrogenolysis becomes significant and it represents the dominant pathway to toluene formation (rather than disproportionation). Furthermore, the highest amount of benzaldehyde produced is provided by hydrogenolysis reaction. However the DH pathway, albeit considerably less influential on benzaldehyde formation, is also present. If this pathway is not considered in the model formulation, a 4% underestimation of benzaldehyde selectivity in the reference experiment would be present.

3.5. Model performance under oxygen-free conditions

One limitation of the proposed model is that step 2 of hydrogenolysis reaction (HL2), leading to toluene formation, strongly depends on the oxygen concentration, and Eq. (59) cannot be used in the total absence of oxygen (oxygen is in the denominator of the direct HL2 reaction). Assuming a very low oxygen concentration is present ($P_{O_2} = 1.0E-5$ bar), the model tends to predict an equimolar distribution of products (Fig. 12b) after several hours when a balance between

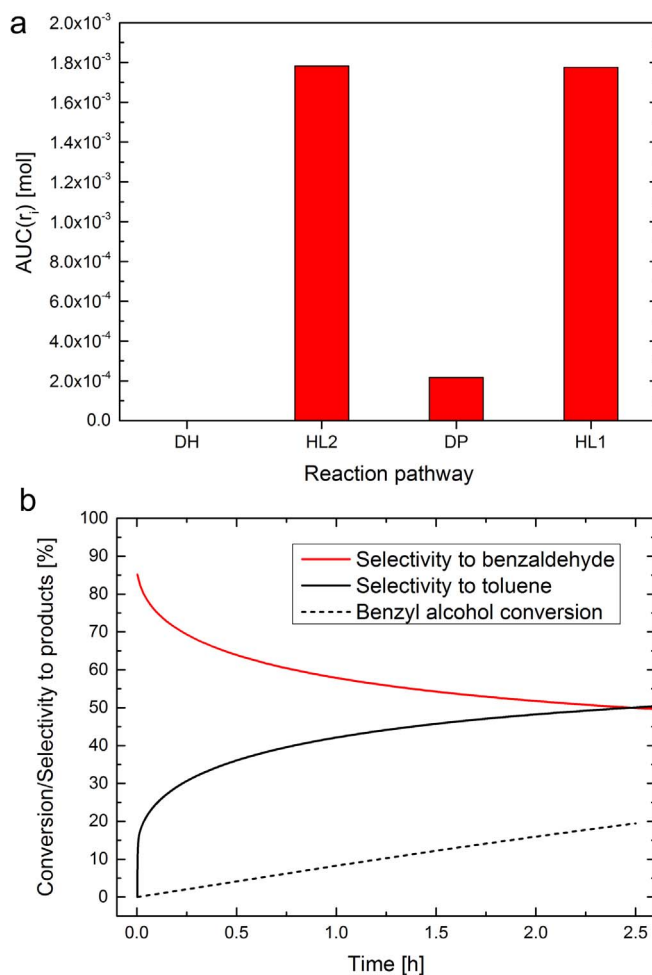


Fig. 12. Model performance under low oxygen concentrations ($T = 80$ °C, $P_{O_2} = 1.0E-5$ bar, $m_s = 1$ g, $m_{cat} = 0.020$ g): (a) analysis of reactions in terms of $AUC(r_i)$; (b) model prediction in terms of conversion and selectivity to products.

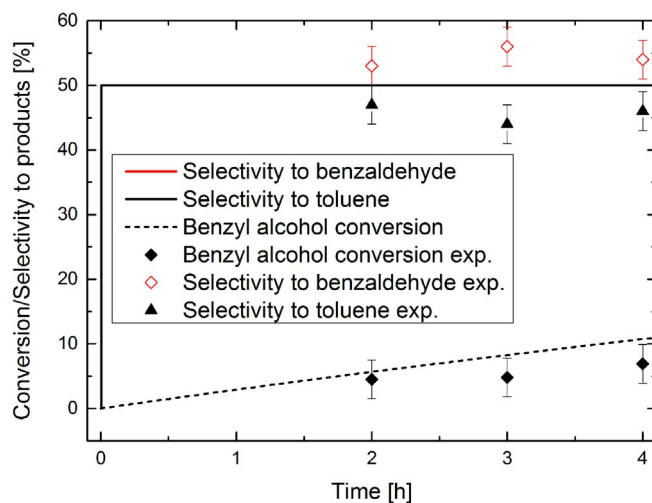


Fig. 13. Model performance under oxygen-free conditions ($T = 80$ °C, $m_s = 1$ g, $m_{cat} = 0.020$ g, $P_{He} = 1$ bar): suppression of HL and DH reactions. Experimental points are indicated by symbols.

HL2 and HL1 pathways is realised (Fig. 12a). As a result of the progressive formation of toluene via HL2, the selectivity to benzaldehyde is relatively high at the beginning of the experiment. Furthermore, a high benzyl alcohol conversion is predicted by the model (around 20% after

2.5 h).

If the kinetic model is used suppressing HL and DH pathways (with the same kinetic constants for the DP reaction reported in Table 5, under the hypothesis of pure disproportionation), an equimolar distribution of products is predicted from the beginning of the experiment (Fig. 13) and, more importantly, a low conversion of benzyl alcohol to products ($X \approx 10\%$) is observed. As becomes apparent from Fig. 13, this is in good agreement with experimental observations obtained in batch experiments [17] where, together with the nearly equimolar distribution of products, a very low conversion ($X \approx 7\%$) was observed after 4 h. These results have also been recently confirmed in flow systems [31] and suggest the existence of a disproportionation-driven mechanism in the absence of oxygen, where hydrogenolysis pathways become negligible. Further experimental investigations are required for modelling in a detailed way the reaction mechanism under oxygen-free experimental conditions.

4. Conclusions

A discrimination procedure was carried out to identify the most suitable kinetic model from a set of chemically-consistent kinetic models for the solvent-free oxidation of benzyl alcohol over Au-Pd/TiO₂. Kinetic models were developed from microkinetic studies based on individual reaction steps starting from the assumption that a number of elementary reactions may take place simultaneously on the catalytic surface. After model simplification in order to preserve the estimability of kinetic parameters from batch data, the most suitable kinetic model for representing the experimental data was found to be a model implementing hydrogenolysis (HL), disproportionation (DP) and dehydrogenation (DH) reactions occurring in parallel. Results showed that the hydrogenolysis reactions cannot be neglected in the model formulation, as this would generate a poor prediction of both conversion and selectivity to benzaldehyde. Despite its relative simplicity, the proposed model was capable of representing the conversion and selectivity to products observed in a stirred batch reactor under different experimental conditions of temperature ($T = 80\text{--}140\text{ }^\circ\text{C}$), pressure ($P_{O_2} = 1\text{--}3\text{ bar}$) and catalyst mass ($m_{cat} = 0.005\text{--}0.080\text{ g}$). A certain degree of uncertainty was present in the experimental measurements at different pressure, but the model was still able to predict an increase in selectivity to benzaldehyde at higher pressures. The same agreement cannot be provided by kinetic models where only direct oxidation and disproportionation reactions are postulated.

The proposed model was used for a quantitative evaluation of each pathway taking place in the reaction system, underlining the important role of temperature on disproportionation and hydrogenolysis reactions. At low temperature the bimolecular kinetics provided by the disproportionation reaction is essential to describe toluene formation, while hydrogenolysis becomes the dominant pathway to toluene at high temperature. The key role of disproportionation for describing the system is even more apparent when oxygen is present at low concentration or is totally absent. Under oxygen-free conditions the model is able to represent the experimental observations of equal distribution of the main products (benzaldehyde and toluene) and a very low benzyl alcohol conversion (even for long reaction times), only if disproportionation becomes the dominant mechanism. Further experimental studies are required to investigate in a more detailed way the kinetic mechanism under these conditions in order to provide a mechanistic description of the complete set of reactions taking place on the catalyst surface.

Acknowledgements

Funding from EPSRC grant (EP/J017833/1) is gratefully acknowledged. We would like to thank the anonymous reviewers for their helpful and insightful comments.

Appendix A. Supplementary data

Supplementary data associated with this article can be found, in the online version, at <http://dx.doi.org/10.1016/j.cej.2017.11.165>.

References

- [1] G.A. Burdock, Fenaroli's Handbook of Flavor Ingredients, 5th ed., CRC Press, London, 2005.
- [2] Y. Perez, R. Ballesteros, M. Fajardo, I. Sierra, I. Hierro, Copper-containing catalysts for solvent-free selective oxidation of benzyl alcohol, *J. Mol. Catal. A: Chem.* 352 (2012) 45–56.
- [3] A. Abad, C. Almela, A. Corma, H. Garcia, Unique gold chemoselectivity for the aerobic oxidation of allylic alcohols, *Chem. Commun.* 17 (2006) 3178–3180.
- [4] K. Mori, T. Hara, T. Mizugaki, K. Ebitani, K. Kaneda, Hydroxyapatite-supported palladium nanoclusters: a highly active heterogeneous catalyst for selective oxidation of alcohols by use of molecular oxygen, *J. Am. Chem. Soc.* 126 (2004) 10657–10666.
- [5] B. Karimi, S. Abedi, J.H. Clark, V. Budarin, Highly efficient aerobic oxidation of alcohols using a recoverable catalyst: the role of mesoporous channels of SBA-15 in stabilizing palladium nanoparticles, *Angew. Chem. Int. Ed.* 45 (2006) 4776–4779.
- [6] Y. Chen, H. Lim, Q. Tang, Y. Gao, T. Sun, Q. Yan, Y. Yang, Solvent-free aerobic oxidation of benzyl alcohol over Pd monometallic and Au-Pd bimetallic catalysts supported on SBA-16 mesoporous molecular sieves, *Appl. Catal. A: Gen.* 380 (2010) 55–65.
- [7] P.J. Miedziak, Q. He, J.K. Edwards, S.H. Taylor, D.W. Knight, B. Tarbit, C.J. Kiely, G.J. Hutchings, Oxidation of benzyl alcohol using supported gold-palladium nanoparticles, *Catal. Today* 163 (2011) 47–54.
- [8] R. Ali, S.F. Adil, A. Al-Warthan, M.R.H. Siddiqui, Identification of active phase for selective oxidation of benzyl alcohol with molecular oxygen catalyzed by copper-manganese oxide nanoparticles, *J. Chem.* 201 (2013) 1–8.
- [9] V.R. Choudhary, D.K. Dumbre, B.S. Uphade, V.S. Narkhede, Solvent-free oxidation of benzyl alcohol to benzaldehyde by tert-butyl hydroperoxide using transition metal containing layered double hydroxides and/or mixed hydroxides, *J. Mol. Catal. A* 215 (2004) 129–135.
- [10] D.I. Enache, J.K. Edwards, P. Landon, B. Solsona-Espriu, A.F. Carley, A.A. Herzing, M. Watanabe, C.J. Kiely, D.W. Knight, G.J. Hutchings, Solvent-free oxidation of primary alcohols to aldehydes using Au-Pd/TiO₂ catalysts, *Science* 311 (2006) 362–365.
- [11] N. Dimitratos, J.A. Lopez-Sanchez, D. Morgan, A.F. Carley, R. Tiruvalam, C.J. Kiely, D. Bethell, G.J. Hutchings, Solvent-free oxidation of benzyl alcohol using Au-Pd catalysts prepared by sol immobilisation, *Phys. Chem. Chem. Phys.* 11 (2009) 5142–5153.
- [12] J.A. Lopez-Sanchez, N. Dimitratos, P. Miedziak, E. Ntainjua, J.K. Edwards, D. Morgan, A.F. Carley, R. Tiruvalam, C.J. Kiely, G.J. Hutchings, Au-Pd supported nanocrystals prepared by a sol immobilisation technique as catalysts for selective chemical synthesis, *Phys. Chem. Chem. Phys.* 10 (2008) 1921–1930.
- [13] E. Cao, M. Sankar, S. Firth, K.F. Lam, D. Bethell, D.K. Knight, G.J. Hutchings, P.F. McMillan, A. Gavriilidis, Reaction and Raman spectroscopic studies of alcohol oxidation on gold-palladium catalysts in microstructured reactors, *Chem. Eng. J.* 167 (2011) 734–745.
- [14] D. Ferri, C. Mondelli, F. Krumeich, A. Baiker, Discrimination of active palladium sites in catalytic liquid-phase oxidation of benzyl alcohol, *J. Phys. Chem. B* 110 (2006) 22982–22986.
- [15] D.I. Enache, D.W. Knight, G.J. Hutchings, Solvent-free oxidation of primary alcohols to aldehydes using supported gold catalysts, *Catal. Lett.* 103 (2005) 43–52.
- [16] T. Mallat, A. Baiker, Oxidation of alcohols with molecular oxygen on solid catalysts, *Chem. Rev.* 104 (2004) 3037–3045.
- [17] S. Meenakshisundaram, E. Nowicka, P.J. Miedziak, G.L. Brett, R.L. Jenkins, N. Dimitratos, S.H. Taylor, D.W. Knight, D. Bethell, G.J. Hutchings, Oxidation of alcohols using supported gold and gold-palladium nanoparticles, *Faraday Discuss.* 145 (2010) 341–356.
- [18] M. Sankar, E. Nowicka, R. Tiruvalam, Q. He, S.H. Taylor, C.J. Kiely, D. Bethell, D.W. Knight, G.J. Hutchings, Controlling the duality of the mechanism in liquid-phase oxidation of benzyl alcohol catalysed by supported Au-Pd nanoparticles, *Chem. Eur. J.* 17 (2011) 6524–6530.
- [19] A. Savara, C.E. Chan-Thaw, I. Rossetti, A. Villa, L. Prati, Benzyl alcohol oxidation on carbon-supported Pd nanoparticles: elucidating the reaction mechanism, *ChemCatChem* 6 (2014) 3464–3473.
- [20] A. Savara, I. Rossetti, C.E. Chan-Thaw, L. Prati, A. Villa, Microkinetic modeling of benzyl alcohol oxidation on carbon-supported palladium nanoparticles, *ChemCatChem* 8 (2016) 2482–2491.
- [21] A. Savara, C.E. Chan-Thaw, J.E. Sutton, D. Wang, L. Prati, A. Villa, Molecular origin of the selectivity differences between palladium and gold-palladium in benzyl alcohol oxidation: different oxygen adsorption properties, *ChemCatChem* 9 (2017) 253–257.
- [22] G.E.P. Box, W.G. Hunter, J.S. Hunter, *Statistics for Experimenters*, John Wiley & Sons, New York, 1978.
- [23] E. Nowicka, J.P. Hofmann, S.F. Parker, M. Sankar, G.M. Lari, S.A. Kondrat, D.W. Knight, D. Bethell, B.M. Weckhuysen, G.J. Hutchings, In situ spectroscopic investigation of oxidative dehydrogenation and disproportionation of benzyl alcohol, *Phys. Chem. Chem. Phys.* 15 (2013) 12147–12155.
- [24] M.J. Ridd, D.J. Gakowski, G.E. Sneddon, F.R. Keene, Mechanism of oxidative dehydrogenation of alcohols co-ordinated to ruthenium, *J. Chem. Soc., Dalton Trans.*

- 12 (1992) 1949–1956.
- [25] S. Vajda, H. Rabitz, E. Walter, Y. Lecourtier, Qualitative and quantitative identifiability analysis of nonlinear chemical kinetic models, *Chem. Eng. Comm.* 83 (1989) 191–219.
- [26] F. Galvanin, C.C. Ballan, M. Barolo, F. Bezzo, A general model-based design of experiments approach to achieve practical identifiability of pharmacokinetic and pharmacodynamic models, *J. Pharmacokinet. Pharmacodyn.* 40 (2013) 451–467.
- [27] G. Wu, E. Cao, S. Kuhn, A. Gavriilidis, A novel approach for measuring gas solubility in liquids using a tube-in-tube membrane contactor, *Chem. Eng. Technol.* 40 (2017) 2346–2350.
- [28] G. Buzzi-Ferraris, F. Manenti, Kinetic model analysis, *Chem. Eng. Sci.* 64 (2008) 1061–1074.
- [29] Process Systems Enterprise, *gPROMS Model Validation Guide (v. 4.1)*. London, Process Systems Enterprise, 2016, 1–72.
- [30] Y. Bard, *Nonlinear Parameter Estimation*, Academic Press, New York, 1977.
- [31] E. Cao, M. Sankar, E. Nowicka, Q. He, M. Morad, P.J. Miedziak, S.H. Taylor, D.W. Knight, D. Bethell, C.J. Kiely, A. Gavriilidis, G.J. Hutchings, Selective suppression of disproportionation reaction in solvent-less benzyl alcohol oxidation catalysed by supported Au–Pd nanoparticles, *Catal. Today* 203 (2013) 146–152.